Title

Evolving SAXS versatility: solution X-ray scattering for macromolecular architecture, functional landscapes, and integrative structural biology

Authors

Brosey, Chris A

Tainer, John A

Publication Date

2019-10-01

DOI

10.1016/j.sbi.2019.04.004

Peer reviewed

HHS Public Access

Author manuscript

Curr Opin Struct Biol. Author manuscript; available in PMC 2020 October 01.

Published in final edited form as:

Curr Opin Struct Biol. 2019 October ; 58: 197–213. doi:10.1016/j.sbi.2019.04.004.

Evolving SAXS versatility: solution X-ray scattering for macromolecular architecture, functional landscapes, and integrative structural biology

Chris A Brosey[1], **John A Tainer**[1,2]

[1]Molecular and Cellular Oncology and Cancer Biology, The University of Texas M. D. Anderson Cancer Center, Houston, TX 77030, USA

[2]MBIB Division, Lawrence Berkeley National Laboratory, Berkeley, CA 94720, USA

Abstract

Small-angle X-ray scattering (SAXS) has emerged as an enabling integrative technique for comprehensive analyses of macromolecular structures and interactions in solution. Over the past two decades, SAXS has become a mainstay of the structural biologist's toolbox, supplying multiplexed measurements of molecular shape and dynamics that unveil biological function. Here, we discuss evolving SAXS theory, methods, and applications that extend the field of small-angle scattering beyond simple shape characterization. SAXS, coupled with size-exclusion chromatography (SEC-SAXS) and time-resolved (TR-SAXS) methods, is now providing high-resolution insight into macromolecular flexibility and ensembles, delineating biophysical landscapes, and facilitating high-throughput library screening to assess macromolecular properties and to create opportunities for drug discovery. Looking forward, we consider SAXS in the integrative era of hybrid structural biology methods, its potential for illuminating cellular supramolecular and mesoscale structures, and its capacity to complement high-throughput bioinformatics sequencing data. As advances in the field continue, we look forward to proliferating uses of SAXS based upon its abilities to robustly produce mechanistic insights for biology and medicine.

Introduction

Structural biology has long interpreted the language of cell biology by illuminating dynamic molecular architectures, revealing how structure encodes biological function and is shaped by genetic sequence and the fundamental physical chemistry underlying evolved molecular mechanisms. The advent of the 'omics' era of biology has significantly expanded the landscape for linking sequence to complex cellular phenotypes via macromolecular shapes, assemblies, and dynamics. Efficient methods to delineate molecular conformations regulating interactions and chemistry in near physiological environments are thus paramount

Corresponding authors: Brosey, Chris A (CABrosey@mdanderson.org), Tainer, John A (JTainer@mdanderson.org).

Conflict of interest statement

Nothing declared.

in this new era of molecular and cellular biology. Following its renaissance over the past two decades, the field of biological small-angle X-ray scattering (SAXS) continues to illuminate biomolecular assemblies and their biophysical states with information-rich experiments, yielding key mechanistic insights into macromolecular functions of cellular machinery. The expansion of dedicated biological SAXS beamlines [1–6], greater use of SAXS combined with crystallography [7••], standardization of publication guidelines for X-ray scattering data [8•,9,10], and development of SAXS data repositories (SASBDB [11•], BIOISIS [www.bioisis.net]) show that SAXS has become an invaluable component of the structural biologist's toolbox.

SAXS is now a robust method for enabling molecular cell biology, providing insight not only into biomolecular shape, but also biomolecular pathway interactions and assembly states, conformational populations within macromolecular ensembles, dynamics of disordered systems, and the evolution of biophysical properties under changing environmental conditions. SAXS remains one of the few structural techniques that can probe macromolecular architecture and dynamics without size limitation under native solution conditions. It furthermore provides multiparameter output on sample quality, particle dimensions and density, and conformational flexibility from a single experiment [7••,12,13•]. Although traditionally considered a low-resolution technique, high-resolution differences in macromolecular conformations can be reliably detected by quantitative comparison of X-ray scattering profiles or SAXS-constrained modeling [14••, 15••, 16]. When combined with high-throughput (HT) sample acquisition, as pioneered by Hura *et al.* [12], the ability to detect and translate conformational trajectories into functional outcomes across multiple size ranges has greatly extended applications of biological SAXS beyond simple shape characterization. Looking ahead, SAXS is emerging as a method to examine the nanoscale of large cellular machineries and their coordinated interactions. Moreover, SAXS is increasingly able to bridge from the nanoscale into the mesoscale of supramolecular interactions, cellular infrastructure, and interactomes, where electrostatic, mechanical, thermal, and bonding energies of macromolecules share similar orders of magnitude [17]. Thus, SAXS is a uniquely versatile and practical HT method, providing a complete, resolution-limited measure of ordered and disordered molecular states, spanning individual protein folds to the subcellular mesoscale.

Here, we present advanced applications of SAXS, which interrogate biophysical properties and states of macromolecules, as well as their structures, allowing functional insight. We first survey recent advances in SAXS data collection and analysis, building upon the SAXS review by Rambo and Tainer [18] and our earlier work defining pathways from crystal structure snapshots [19]. From there, we examine how SAXS can characterize macromolecular flexibility and conformational ensembles, uncover biophysical landscapes, and enable applications in HT screening, extending from ligand and co-factor binding to frontiers in drug discovery. We conclude by considering SAXS in the emergent integrative era of structural and molecular biology, where multiple and increasingly sizeable data sets are coming to bear on complex subcellular structures and where the available structural landscape itself is expanding with the rise of genomic information [20].

SAXS essentials - one experiment, many measurements

In its most basic form, the biological SAXS experiment captures the pattern of X-rays scattered from the electrons that compose a macromolecular solution. The important angular range for shape information on biological macromolecules typically lies between 0.03° and 5° and is best captured by placing a detector 1.5 m or more away from the sample. The particle scattering intensity, $I(q)$, is a function of all inter-atomic (electron-pair) distances contained within a macromolecule:

$$I(q) = 4\pi \int_0^{D_{max}} P(r) \frac{\sin(qr)}{qr} dr \quad (1)$$

where r is the distance between electron pairs within the macromolecule and $D_{\max}$ is the maximum of these distances [7••] (Figure 1). Scattering intensity is a function of the momentum transfer, q:

$$q = \frac{4\pi \sin(\theta)}{\lambda} \quad (2)$$

where 2θ is the scattering angle relative to the path of the X-ray beam, and λ is the X-ray wavelength (Figure 1). Importantly, the momentum transfer q, reported in $Å^{-1}$ (UK/US) or nm^{-1} (EU), defines the scattering curve in reciprocal space independent of detector distance and wavelength (λ).

Once a measured scattering curve has been corrected for buffer scattering, mathematical transformations of $I(q)$ (implemented in standard SAXS analysis packages [21••,22], https://bll231.als.lbl.gov/scatter/) yield information on molecular geometry and sample integrity.

Key examples of these analyses include the Guinier approximation of the low-q region of the scattering curve to estimate the radius-of-gyration (R_g), assessment of the Porod volume (V_p) of the molecular scattering envelope, Fourier transformation of $I(q)$ to yield the real-space pair-distance distribution of the macromolecule, $P(r)$, and Kratky transformation, which provides a qualitative assessment of the compactness or flexibility of the scattering particle [7••, 16] (Figure 1b, c). Guinier analysis of the low-q scattering signal can also detect sample aggregation and radiation damage, reflected as non-linearity within the Guinier transform and a rise in R_g and $I(0)$ (the extrapolated zero-angle scattering intensity) with increasing exposure time.

Moving toward higher signal and experimental throughput

While scattering experiment essentials have not changed, advances in measurement speed and sensitivity are proving to be game changers. In tandem with the detector revolutions in X-ray crystallography and electron cryomi-croscopy (cryoEM), direct photon detectors at SAXS beamlines have improved detection of weak scattering signals from dilute and limited samples while reducing exposure and consequent radiation damage [2,23,24]. A lack of

detector dark current and lowered readout noise improves baseline stability and reduces recorded noise within the scattering curve, enabling sample concentrations of 0.5–1.0 mg/mL. The direct detection of X-ray photons, combined with advances in detector readout technology, permits readout rates within the millisecond regime. Increased data collection speed allows shorter, more frequent exposures of SAXS samples, mitigating radiation damage effects and allowing users to utilize early damage-free frames for merging and analysis (sibyls.als.lbl.gov/ran). With the new detectors, virtually every SAXS experiment can essentially become a time-resolved experiment at synchrotron beamlines, and sample solutions can be directly monitored as they emerge from size-exclusion chromatography.

Improvements in sensitivity and readout provided by direct detectors and innovations in capillary sample flow cells have spurred the rapid rise of size-exclusion chromatography coupled (SEG)-SAXS [25•,26] and time-resolved (TR)-SAXS [27•,28,29]. The advent of SEG-SAXS allows spatial separation according to size, whereas continued improvements in TR-SAXS enable temporal separation of changes in conformation and assemblies. SEG-SAXS applications have proved particularly powerful in isolating monodisperse species from polydisperse or aggregating samples, thereby yielding structural information on transient macromolecular conformations and complexes inaccessible by static observation (*infra vide*). Moreover, combining SEG-SAXS with singular value decomposition (SVD) methods, such as Evolving Factor Analysis (EFA) [30•], can yield unique scattering profiles from co-eluting species. The increased ability to automate buffer equilibration and sample loading is guiding SEG-SAXS toward the high-throughput regime.

TR-SAXS experiments capture transient and evolving macromolecular conformations occurring on timescales of microseconds to days. The exact time resolution depends upon the trigger initiating macromolecular changes, whether laser irradiation (light), pressure or temperature jumps, or most commonly, microfluidic mixing with continuous or stopped-flow devices [27•]. TR-SAXS coupled with rapid mixing can monitor biomolecular transitions occurring on timescales of microseconds to milliseconds. While sample consumption remains high for TR-SAXS, a single experiment can capture multiple states along a conformational trajectory, yielding critical kinetic insights into biological processes.

Conventional SAXS has become a true HT structural technique with advances in automated sample handling, sample cell design, and sample preparation. Synchrotron SAXS beamlines have now demonstrated acquisition rates of 30–60 min per 96-well plate (http://bll231.als.lbl.gov/) [2,31], allowing screening experiments to take place in conjunction with structural characterization. Currently, sample cell washing occupies the highest percentage of a plate's acquisition time, and parallelized sample loading and washing is expected to lower acquisition rates by half or further. While standard liquid handling robotics can be used to prepare 96-well plates for HT-SAXS, microfluidic sample platforms, such as the LabDisk for SAXS and Photonic Lab-on-a-Chip, are an active area of development to reduce sample volume and preparation time [32,33]. These devices allow rapid multiplexing of buffer and screening conditions concurrently with preparation of sample dilution series, using minimal material (2.5 μL for LabDisk). Continued innovation in microfluidic sample devices is expected to further enable SAXS as a technology for mainstream HT screening.

HT approaches to SAXS analysis

As SAXS has entered the HT era, approaches for assessing and interpreting large-scale SAXS data sets are critically needed. Data quality evaluation and analysis have traditionally required time-intensive manual processing and assessment. Thus, the emergence of automated, on-line data analysis pipelines to assess, process, and analyze multi-sample data sets are critical [34,35] (https://www-ssrl.slac.stanford.edu/~saxs/analysis/saxspipe.htm). The robustness of high-throughput data assessment has been examined using the *SAXSstats* protocol of Grant *etal.* [34]. The SAXS analysis program Atsas also includes a high-throughput analysis module SAS-FLOW, which can move SAXS data from background subtraction to modeling [35].

For distinguishing $I(q)$ differences in a screening context, rapid and robust methods are key for comparing and detecting differences among a population of scattering profiles. The volatility-of-ratio (V_R) parameter developed by Hura *et al.* [14••] assesses differences for the normalized, binned ratio of two scattering curves, $R(q)$, where $R(q) = I(q)_1/I(q)_2$ This provides a robust metric for pairwise comparison of scattering curves across the entire resolution range of scattering vectors to define structural similarity objectively (Figure 2). Although valuable, classic pairwise difference metrics, such as $\chi 2$ and the Pearson correlation coefficient, give increased weight to low-resolution regions of $I(q)$. In contrast, ratiometric V_R offers even weighting of the entire q-range and is thus sensitive to differences at both high and low q-values, more effectively detecting sample differences on multiple distance scales. Having calculated V_R for a population of scattering curves, the resulting V_R values can be efficiently assembled, clustered, and assessed for trends using a SAXS similarity matrix (https://bll231.als.lbl.gov/saxs_similarity/). This HT, population-level approach to SAXS analysis is robust and objective for a wide range of biological problems, from ligand-induced allosteric states [36] to DNA repair enzyme conformations[14••].

Expanding the SAXS analysis and modeling toolbox

As SAXS experimental set-ups have continued to evolve and develop, SAXS theory and analytical approaches have made similar advances, particularly for the characterization of flexibility and dynamics in biomolecular systems. Although some information on flexibility may be obtained in X-ray crystallography from temperature factors corrected for crystal contacts [37], SAXS directly measures flexibility in solution. Detecting flexibility not only provides insight into molecular architecture and structural changes, but also guides the choice of rigid-body or population-based ensemble approaches when generating molecular models with pre-existing high-resolution structures. Flexibility analysis is also critical for determining whether classical *ah initio* shape reconstruction, implemented by programs such as DAMMIN [38] and GASBOR [39], is appropriate for a system.

The development of the Porod-Debye interpretation of flexibility with Kratky-Debye [$q^2 \cdot I(q)$], SIBYLS [$q^3 \cdot I(q)$], and Porod-Debye [$q^4 \cdot$(Iq)] plots and their corresponding quantitation by the Porod exponent (P_E) have enabled objective, quantitative assessment of molecular flexibility and compactness [40••,·41] (Figures lc, 2b). The presence or absence of a plateau in these three power transforms of the scattering curve $I(q)$ are assessed to

diagnose flexibility. Rigid, well-defined macromolecules exhibit defined plateaus in the Porod-Debye transform [$q^4 \cdot$(Iq)]. Intrinsically disordered systems exhibit plateau formation in the Kratky-Debye plot [$q^2 \cdot I(q)$]. The SYBILS plot [$q^3 \cdot I(q)$] presents a plateau for systems containing a mixture of rigid and flexible elements, such as flexible, multi-domain proteins. The Porod exponent provides a quantitative measure of the qualitative behavior observed in flexibility plots, assuming values of 2–4 for fully flexible to fully compact systems, respectively.

The recently defined volume-of-correlation (V_c) parameter is the first SAXS invariant to be discovered since the Porod invariant sixty years ago [42••]. It is calculated as a scaled ratio of particle volume (V_p) and self-correlation length (l_c) and provides complementary monitoring of changes in molecular conformation for flexible systems [42••]. When comparing two matched scattering profiles (i.e. receptor with and without ligand), increases in V_c are reflective of decreased compactness and increased flexibility, and vice-versa. Pairing V_c with the radius-of-gyration to form the power-law parameter $Q_R\left(V_c^2/R_g\right)$ critically enables direct determinations of hydrated molecular mass of compact and flexible SAXS samples without the need for absolute scaling calibrations [42••]. Such concentration-independent methods to assess biomolecular mass are invaluable for discriminating among scattering changes arising from sample assembly formation versus conformational rearrangement [42••,43,44•].

The presence of conformational flexibility in a SAXS sample should steer modeling efforts toward ensemble approaches for flexible systems, when pre-existing high-resolution structures are available (reviewed in the next section). When high-resolution structures are unavailable and flexibility analysis indicates structured macromolecular flexibility, a recently developed *ab initio* shape reconstruction program, DENSS, may provide low-resolution insight into macromolecular architecture. Traditional *ab initio* shape reconstruction programs, such as DAMMIN and GASBOR [39,45,46], optimize placement of spherical beads within a fixed volume restrained by D_{max} relative to the $I(q)$~derived $P(r)$ distance distribution, creating a low-resolution shape envelope reflecting macromolecular architecture. Modeling of flexible biomolecules by these *ab initio* methods often fails, however, from penalty restraints requiring a compact model and uniform density.

DENSS (DENsity from Solution Scattering) applies iterative structure factor retrieval directly to experimental scattering data to produce low-resolution electron density volumes [47•]. Its advantage over current *ab initio* shape reconstruction algorithms lies in capturing non-uniform biomolecular volumes (e.g. particle cavities) and detecting differences in electron density among different biomolecular phases (e.g. protein versus lipid). Because it allows for non-uniform electron density, DENSS may improve modeling of flexible and disordered systems. A key need for all *ab initio* reconstruction algorithms is full utilization of $I(q)$ information from the high-q region (q > 0.2 Å). As $I(q)$ spans two orders of magnitude (10^2) across q space (Figure 1), noise has the greatest impacts on low signal in the high-q region. Consequently, low angle $I(q)$ with high intensity and low noise dominates *ab initio* reconstructions, leaving lower intensity, noisier, high-q data underutilized. As the

high-*q* signal is being measured with increasing accuracy, this higher resolution data could extend the detail and resolution of *ab initio* models.

Continued developments in *ab initio* modeling have also examined questions of uniqueness and resolution for shape reconstructions. The *ATSAS* analysis module AMBIMETER provides a new aid to assess shape ambiguity before the calculation of the shape reconstruction by determining the uniqueness of the experimental scattering profile relative to a library of shape skeletons [48•]. SAXS data exhibiting unique topological shape information are more likely to produce unambiguous *ab initio* modeling results. SASREF, also from *ATSAS*', utilizes the average Fourier shell correlation (FCS) function across a set of *ab initio* envelope solutions to generate an estimate of envelope resolution and thus a quantitative benchmark for comparing envelope reconstructions from different SAXS curves [49•].

Structural dynamics: capturing functional biomolecular flexibility

SAXS can access both well-defined macromolecular architecture and flexible dynamics simultaneously, revealing functional conformations and dynamics often invisible to static approaches, such as X-ray crystallography and cryoEM. It also captures the complete architecture of the biologically relevant solution ensemble, in contrast to other site-specific solution techniques (NMR, FRET, EPR), which may selectively report from very specific regions of a biomolecule. Multiple approaches are available to model dynamic conformational ensembles encoded in the scattering curve. Current ensemble modeling programs include EOM (Ensemble Optimization Method) [50,51], Minimal Ensemble Search (MES) partnered with BILBOMD [52] or MultiFoXS (Multi Fast X-ray Scattering) [53,54], EROS (Ensemble Refinement of SAXS) [55], and BSS-SAXS (Basis-Set Supported SAXS) [56] (Figure 2c). These programs utilize different approaches to generate starting ensembles for refinement against SAXS data. These include high-temperature, implicit-solvent molecular dynamics on domain linkers (BilboMD), knowledge-based sampling (EOM, MultiFoXS), and coarse-grain molecular dynamics (BSS-SAXS, EROS). Each program has unique advantages to modeling different kinds of biomolecular ensembles. EOM shows success in modeling biomolecular systems with highly fluctuating structures, such as intrinsically disordered proteins (IDPs) [57,58] and RNAs [59]. BILBOMD-MES is optimized for flexibly linked, multi-domain systems or rigid domains with flexible loops or termini [60,61], as are EROS [62,63] and BSS-SAXS [56]. MultiFoXS and its MES approach are targeted toward modeling conformational heterogeneity within well-defined molecules, such as immunoglobulin chains [64,65•].

Ensemble modeling approaches have proved critical to revealing the properties of dynamic functional states. Recent scattering studies have probed functional conformations in cytoskeletal actin-binding protein adseverin [66], assemblies from the mammalian circadian clock [67], intrinsically disordered proteins tau and a-synuclein [68,69••], multi-domain bacterial carboxylic acid reductase [70] and outer-membrane protein (OMP) chaperone Skp [71], ubiquitin-modified and SUMO-modified PCNA [72,73], dynamic complexes of the non-homologous end-joining (NHEJ) DNA double-strand break repair pathway [57,74,75••] DNA conformations in DNA mismatch repair [76], and nucleosome unwrapping [77••,78].

Moreover, ensemble approaches are significantly extended in their application when combined with SEG-SAXS and TR-SAXS experiments. Combined application of ensemble modeling and SEC-SAXS was essential to characterizing the solution architectures of Ku/DNA-PKcs/APLF and Ku/XRCC4/DNA Ligase IV/APLF assemblies, which orchestrate NHEJ repair [75••]. Studying intact complexes bound to DNA substrate with SEC-SAXS permitted the detection and isolation of scattering signal from stably associated, nonaggregating complexes. Subsequent modeling of the complex was aided by ensemble modeling of intrinsically disordered APLF and the flexibly attached C-terminal domain of Ku80 using BILBOMD-MES. Besides capturing 'instantaneous' molecular ensembles, ensemble modeling is increasingly used to monitor evolution of ensembles over time via TR-SAXS. The elegant exploration of nucleosome unwrapping by Chen and colleagues used such ensemble methods to deconvolute DNA conformational changes over progressing SAXS snapshots and to construct kinetic pathways for nucleosome disassembly [77••, 78]. Their study also cleverly capitalized upon sucrose contrast-matching of the sample buffer to minimize the scattering signal from protein histones and to maximize the DNA scattering signal for analysis. Similarly, Plumridge *et al.* tracked the progression of magnesium-induced conformational collapse for the tP5abc three-helix junction RNA with TR-SAXS and ensemble fitting from molecular dynamics snapshots [79••].

While ensemble methods provide realistic representations of solution conformations, their ability to describe ensembles is often constrained by limitations in fully sampling the available conformational space for subsequent screening against SAXS data. Coarse-grained (CG) and all-atom (AA) molecular dynamics simulations, computed with implicit or explicit solvation, are being used with rising frequency to increase conformational sampling and to aid the interpretation of scattering data [62,73,80–83]. With their reduced particle number and degrees-of-freedom, coarse-grained approaches enable broad and rapid conformational sampling of collective macromolecular motions with a streamlined computational load [84]. At the same time, recent advances in parallelization with GPU (graphics processor unit) technology have made the extended periods of AA simulations (sub-microseconds and longer) accessible to desktop computers. Notably, application of sampling enrichment strategies (accelerated MD, amplified collective motions) are also improving conformational pools for SAXS-driven ensemble selection [85,86].

An innovation in ensemble modeling driven by both GG and AA MD simulations applies the experimental SAXS curve as an energetic restraint in structure sampling and refinement, rather than a comparative reference or a postsampling filter for conformational selection [15••,83,87,88] (Figure 2). Hybrid refinement methods, such as those that combine NMR and SAXS data [89,90•,91], use a similar approach by incorporating a SAXS-fitting term into existing NMR-parameter driven scoring functions. Chen and Hub, however, present a direct refinement method with small-angle and wide-angle scattering data (SAXS/WAXS), using explicit-solvent molecular dynamics (MD) simulations to evolve crystallographic starting models (SWAXS-driven MD) [15••]. Their SAXS-guided sampling ensures adequate exploration of the relevant conformational space, while their application of explicit solvent avoids inaccuracies from fitting of the solvent layer and excluded volume, thereby achieving better modeling of higher-resolution wide-angle scattering data. The use of molecular

dynamics to model a more accurate solvent layer is also employed by *WAXSiS* [92•], which computes theoretical scattering curves from fixed atomic PDB coordinates.

As use of SAXS-guided structural refinement and explicit modeling of macromolecular hydration becomes mainstream, testing how higher-resolution data from wide-angle scattering experiments impacts and improves knowledge of structures and conformational dynamics will be valuable, especially for parsing high-resolution scattering contributions from atomic thermal motions [93]. Conversely, SAXS-guided insights from biomolecular and solvent dynamics may aid in bridging the 'R-factor gap' for correlating crystal structures with X-ray diffraction data [94]. Hybrid refinement methods, which utilize multiple sources of structural information (X-ray crystallography, NMR, SAXS, cryoEM) are also poised to benefit from advances in SAXS-based modeling and refinement strategies.

Probing biophysical landscapes

Beyond establishing functional dynamic structures, SAXS is now a key technology for investigating functional biophysical properties. Biomolecular shape and flexibility encode thermodynamic information, reflective of their folded, multi-conformer, or disordered states, and can be monitored for state changes (Figure 3). SAXS R_g and *P(r)* measurements are increasingly used for proteins [95–100,101•] and RNA [41,102–108] to construct temperature and ion-dependent phase diagrams and reaction coordinates for folding. Protein energy landscapes can be assimilated from or validated by SAXS data [109,110]. TR-SAXS accesses biomolecular reaction and pathway intermediates, as exemplified by studies of virus capsid maturation [111], the photocycle of photoactive yellow protein (PYP) [29], and nucleosome disassembly [77••], allowing extraction of kinetic information and delineation of conformational trajectories. Notably, the ability to detect and quantify populations of individual species and their complexes within scattering data can reveal thermodynamic interactions among binding partners.

A unique application of multi-species population modeling was reported by Gordeiro *et al.* and provided an analysis framework for using SAXS titration series to monitor and model transient, multi-species interactions, in this case, DNA damage response factor PGNA and its disordered regulatory binding partner $pl5^{PAF}$ [112••]. Their study used explicit-solvent MD simulations to model the free binding partners and three potential interaction stoichiometries, from which ensemble-averaged SAXS curves were generated. By use of the ensemble-averaged SAXS curves as a basis set, they globally fitted the experimental scattering data collected across a $pl5^{PAF}$/PCNA titration series to deconvolute fractional binding populations and estimate the K_d. Their approach simultaneously quantified concentration-dependent population distributions of $pl5^{PAF}$/PGNA complexes, while illuminating the heterogeneous architecture of each complex.

Mapping dynamic landscapes of protein-DNA complexes by SAXS has benefited from selective labeling with heavy elements that scatter more strongly than protein or DNA. The average electron density of gold nanocrystals is ~4.6 electrons/$Å^3$ compared to 0.44 electrons/$Å^3$ for protein or 0.55 electrons/$Å^3$ for DNA. For biological SAXS experiments, the scattering signal is scaled by the square of the electron density difference between the

scattering object and water (0.33 electrons/Å^3). Thus, the zero-angle scattering intensity for a gold particle is 1650-fold greater than a protein of equivalent size. With mathematical treatments of gold nanocluster scattering in place [76], their > 1000-fold increased scattering offers powerful opportunities to examine specific distances in complex mixtures. For example, Hura *et al.* successfully used gold-labeled DNA substrates to probe conformational changes on the DNA induced by the *E. coli* mismatch repair factors MutS and MutL. These experiments enabled them to propose a mechanism for base-mismatch recognition, in which the substrate DNA is initially distorted, and then straightened as repair complexes migrate on the DNA.

SAXS can also robustly detect, deconvolute, and quantify kinetic progression of macromolecular aggregation and assembly processes, often associated with significant human diseases. Destabilizing hotspot patient mutations in glycine 93 of Gu, Zn superoxide dismutase (SOD) result in amyotrophic lateral sclerosis (ALS). However, the SOD mutant crystal structures were very similar to the wild-type protein. Nevertheless, SAXS revealed an increased propensity of the mutant enzyme toward aggregated filament formation in solution, corresponding with the clinical severity of ALS [113]. In a similar manner, time-resolved SAXS coupled with a novel data deconvolution approach, COSMiCS (Complex Objective Structural Analysis of Multi-Component Systems), probed amyloid formation by insulin and the E46K α-synuclein Parkinson's disease mutant [69••]. In this application, COSMiCS was used to extract component scattering profiles for an evolving mixture of species (monomer, oligomer, fibril). Experimental *I(q)* scattering profiles collected during the aggregation process and combinations of their mathematical transforms (Holtzer $q \cdot I(q)$; Kratky $q^2 \cdot I(q)$; Porod $q^4 \cdot I(q)$) were used as inputs. The inclusion of the *I(q)* transforms, which emphasize different distance scales encoded in the experimental $I(q)$ curves, proved important for isolating scattering curves from species along the aggregation trajectory and for estimating their relative populations. Continued innovation in TR-SAXS, as well as SEC-SAXS, will enable further exploration and development of biophysical applications for insight into fundamental biochemical processes and human pathologies.

HT screening with SAXS: current and emerging applications

HT data collection platforms have spurred the expansion of screening applications using SAXS [114]. Current among these are rapid validation of protein engineering design targets [101•,115–118], micro-screening of macromolecular crystallization conditions [119,120], characterization of protein mutant/variant libraries [36,113,121–123], profiling ligand/metabolite binding [14••], assaying for protein-RNAand protein-ligand interactions [14••, 124], and assessing antibody formulations [125–127]. SAXS offers the dual benefit of facilitating screening endpoints in solution, while providing multi-parameter architectural read-outs on each system.

SAXS has proved increasingly significant for synthetic biology, facilitating efficient design and optimization of nanoscale biological materials. For example, SAXS was used to screen self-assembling cyclic homo-oligomers and to link nanoscale architecture with rational design of protein interfaces [117]. In a similar manner, SAXS determined conformational classifications of self-assembling protein cages and interrogated cage stability under a range

of solvent, pH and salt conditions [101•]. Notably, these authors created a custom, theoretical conformational landscape for benchmarking their cage designs with SAXS. Conformational snapshots were generated by a Chimera morph between compact and symmetrically open cage structures. The authors then simulated SAXS curves for these conformational snapshots and used this conformational benchmark to interpret the experimental impact of exposing protein cages to varying solvent conditions. Their analysis made use of simultaneous plotting of theoretical and experimental data in V_R similarity matrices and force plots, which represented each dataset as a node and scale distance between nodes according to V_R similarity (https://bll231.als.lbl.gov/saxs_similarity/). This ability to compare and rapidly assess biomolecular materials against targeted designs positions SAXS to play a key role in the design cycle of nanoscale bioengineering.

In the same way, HT-SAXS assessments have and will continue to provide feedback on macromolecular targets traversing protein biochemistry and crystallography pipelines. Success in protein crystallography relies first upon effective construct design, and SAXS provides a ready means for determining and selecting stable protein constructs from prepared libraries, identifying constructs which minimize aggregation and internal flexibility. SAXS is also well positioned to identify optimum solvents to support protein construct stability once a construct has been selected. The recent demonstration of SAXS's ability to measure second virial coefficients for varying lysozyme and salt concentrations on a microfluidic chip [119] is further support for the potential of SAXS to aid in identifying conditions favorable for crystallization.

While SAXS has found diverse HT applications, it still remains underutilized in arenas of small-molecule screening and drug discovery. Nevertheless, SAXS excels in detecting ligand impact on macromolecular structure: the formation, perturbation, and disruption of protein complexes; allosteric rearrangement of protein domains; and enhanced or restrained polypeptide flexibility. Examples of physiologic small-molecule ligand interactions accessible by SAXS have included receptor-ligand binding [128], co-factor interactions [36,129], metal ion binding [130], and UV photo sensing [131]. Moreover, ensemble readout from SAXS is well suited to detecting selective stabilization of transient conformations by ligand interactions. Development of allosteric modulators of protein ensembles has come increasingly into focus for drug targeting, as these ligands avoid competitive interplay with endogenous ligands [132–134]. The move to target small-molecules toward protein complexes and assemblies to more effectively modulate signaling pathways is well aligned to these advantages of SAXS-based approaches for screening and structure-function analysis. As the useful resolution range of the scattering curve expands, SAXS may find a place in providing read-out of subtle target-ligand interactions.

The integrative structural biology era

The twenty-first century has heralded the integrative era of structural biology, where comprehensive descriptions of macromolecular architecture and function are assembled from multiple, complementary structural techniques [135–137]. For many years, SAXS has extended conformational and oligomeric information from atomic resolution crystal structures [138–142], aided NMR-driven structural refinement and model-building [82,89–

91,143–149], provided global read-out to complement NMR dynamics measurements [150], enabled visualization of protein complexes from crystallized or computationally modeled components [151,152], and informed *ab initio* protein fold modeling [99•]. With improved methods for integrative computational modeling [153,154••,155••], advances in native and cross-linking mass spectrometry (MS) analysis [156–158], integration with single-molecule methods [159], and the emergence of the cryoEM revolution [160,161], SAXS is primed to provide integrative conformational information for large macromolecular assemblies *in vitro*, as well as biological complexes studied *in situ* by cryo-soft X-ray and cryo-electron tomography [162–164] (Figure 4).

Complementary validation and interpretation of macromolecular assemblies from cryoEM or cryo-tomographic methods using SAXS data are already mainstream [165–168]. Global metrics for evaluating integrative structural models generated from SAXS and complementary data sets, however, remain rare. Multi-data refinement platforms, such as the Integrative Modeling Platform (IMP), have developed tools for synthesizing multiple sources of spatial restraints to drive model-building and refinement [155••,169,170], and efforts by the world wide Protein Data Bank (wwPDB) and others have begun to lay groundwork for the curation and validation of integrative/hybrid structural models [171•, 172]. While efforts by platforms such as IMP have made impressive headway in bringing diverse data sources to bear on hybrid models, a key advance remains to be made in the pursuit and development of confidence-weighted multi-data refinement methods to capitalize upon the common structural information encoded in X-ray crystallography, cryoEM, and SAXS data.

Looking toward the future, structural biology is poised to extend the pursuit of macromolecular assemblies and machinery to nanoscale and mesoscale cellular structures. Notable recent examples have included the impact of Tau variants on microtubule crowding [173], the architecture of nucleosome fibers [174•, 175], and bacterial nucleoid compaction [168•]. With time-resolved methods, SAXS has the potential to investigate the biochemical determinants of more dynamic supramolecular assemblies, such as phase-driven coalescence of chromatin subcompartments [176], nucleation of stress granules [177], and diffusion recovery of DNA repair foci. These novel phase separations may entail Turing pattern formation and could be examined by SAXS analytics such as V_c, which reports on voids within assemblies [42••]. Such dynamic biomolecular condensates represent a frontier for extending SAXS into the study of cellular structures, linking nanoscale and mesoscale in cell biology. In a similar manner, the exponential increase in genomic sequencing data across species and disease states also presents opportunities and challenges for extracting structural information to aid in predicting phenotypic outcomes. Here, SAXS can link important human protein targets to accessible yeast and bacterial model protein systems to inform human molecular biology and disease [178]. Combining such approaches with rapid HT-SAXS analyses can provide opportunities for translating disease-specific and species-specific variations in target sequences into libraries of three-dimensional architectural information, reporting on functional variation that can be leveraged for diagnostic output.

SAXS: today and future horizons

The past two decades have established biological X-ray scattering as a mainstay of structural biology and expanded the paradigm for interpreting macromolecular function through supramolecular architecture. SAXS is well established in revealing the shape, conformations and assemblies of biological systems. As the field continues to evolve and illuminate complex biological problems, novel applications of HT-SAXS, SEC-SAXS, and TR-SAXS will extend the spatial and temporal resolving power of this technique even further. Biological SAXS has and will continue to capitalize upon computational advances to drive interpretation of scattering data towards higher resolution and further insight into macromolecular shape, assembly states, flexibility, and conformational ensembles. SAXS has also become a powerful tool for tracking biophysical states associated with folding, unfolding, and aggregation and for assaying biochemically relevant ligand interactions. The HT scale of SAXS has facilitated its use in biotechnological applications, such as synthetic biology and protein construct screening, and is well positioned to aid in drug discovery and diagnostic structure-function analyses of disease-causing and cancer-causing mutations. Looking forward to the ‘SAXS revolution’ over the next decade, we anticipate that biological X-ray scattering will continue to be a driver in integrative structural biology, empower investigation of nanoscale/mesoscale cellular structures, and sustain a role in mapping novel and dynamic functional architectures from the global genome.

Acknowledgements

Our work on SAXS analysis is supported by National Institutes of Health (NIH) grants (P01 CA92584, R35 CA220430), the Cancer Prevention and Research Institute of Texas (RR140052 and RP180813), and the University of Texas System Science and Technology Acquisition and Retention. Our SAXS facilities and technologies are supported by the Department of Energy, Office of Basic Energy Sciences, Integrated Diffraction Analysis Technologies (IDAT) program, and the NIH P30 GM124169. J.A.T. is supported by a Robert A. Welch Chemistry Chair. We thank Drs Greg Hura, Susan Tsutakawa, James Holton, Michal Hammel, Scott Classen, and Aleem Syed for discussions and useful input.

References and recommended reading

Papers of particular interest, published within the period of review, have been highlighted as:

• of special interest

•• of outstanding interest

1. Classen S, Hura GL, Holton JM, Rambo RP, Rodic I, McGuire PJ, Dyer K, Hammel M, Meigs G, Frankel KA et al.: Implementation and performance of SIBYLS: a dual endstation small-angle X-ray scattering and macromolecular crystallography beamlineatthe Advanced Light Source. J Appl Crystallogr 2013, 46:1–13. [PubMed: 23396808]
2. Blanchet CE, Spilotros A, Schwemmer F, Graewert MA, Kikhney A, Jeffries CM, Franke D, Mark D, Zengerle R, Cipriani F et al.: Versatile sample environments and automation for biological solution X-ray scattering experiments at the P12 beamline (PETRA III, DESY). J Appl Crystallogr 2015, 48:431–443. [PubMed: 25844078]
3. Pernot P, Round A, Barrett R, Antolinos AD, Gobbo A, Gordon E, Huet J, Kieffer J, Lentini M, Mattenet M et al.: Upgraded ESRF BM29 beamline for SAXS on macromolecules in solution. J Synchrotron Radiat 2013, 20:660–664. [PubMed: 23765312]

4. Zeng JR, Bian FG, Wang J, Li XH, Wang YZ, Tian F, Zhou P: Performance on absolute scattering intensity calibration and protein molecular weight determination at BL16B1, a dedicated SAXS beamline at SSRF. J Synchrotron Radiat 2017, 24:509–520. [PubMed: 28244448]

5. Acerbo AS, Cook MJ, Gillilan RE: Upgrade of MacCHESS facility for X-ray scattering of biological macromolecules in solution. J Synchrotron Radiat 2015, 22:180–186. [PubMed: 25537607]

6. Allaire M, Yang L: Biomolecular solution X-ray scattering at the National Synchrotron Light Source. J Synchrotron Radiat 2011, 18:41–44. [PubMed: 21169689]

7. Putnam CD, Hammel M, Hura GL, Tainer JA: X-ray solution scattering (SAXS) combined with crystallography and computation: defining accurate macromolecular structures, conformations and assemblies in solution. Q RevBiophys 2007, 40:191–285.•• Classic treatise on biological X-ray scattering and crystallography. Putnam et al. examine SAXS theory and experimental strategies and describe applications for integrating SAXS, crystallography, and computational tools to model macromolecular complexes and flexibility.

8. Trewhella J, Duff AP, Durand D, Gabel F, Guss JM, Hendrickson WA, Hura GL, Jacques DA, Kirby NM, Kwan AH et al.: 2017 publication guidelines for structural modelling of small-angle scattering data from biomolecules in solution: an update. Acta Crystallogr D Struct Biol 2017, 73:710–728. [PubMed: 28876235] • The International Union of Crystallography (lUCr) Small-Angle Scattering and Journals Commissions, Small-Angle Scattering Validation Task Force of the Worldwide Protein Data Bank (wwPDB), and additional experts in the field of biological scattering outline publication guidelines and recommendations for SAXS sample quality, data processing, and data analysis, validation, and modeling.

9. Jacques DA, Guss JM, Svergun Dl, Trewhella J: Publication guidelines for structural modelling of small-angle scattering data from biomolecules in solution. Acta Crystallogr D Biol Crystallogr 2012, 68:620–626. [PubMed: 22683784]

10. Trewhella J, Hendrickson WA, Kleywegt GJ, Sali A, Sato M, Schwede T, Svergun Dl, Tainer JA, Westbrook J, Berman HM: Report of the wwPDB Small-Angle Scattering Task Force: data requirements for biomolecular modeling and the PDB. Structure 2013, 21:875–881. [PubMed: 23747111]

11. Valentini E, Kikhney AG, Previtali G, Jeffries CM, Svergun DI: SASBDB, a repository for biological small-angle scattering data. Nucleic Acids Res 2015, 43:D357–D363. [PubMed: 25352555] • Valenti et al. describe implementation of the small-angle scattering biological data bank (SASBDB) (www.sasbdb.org), a repository for small-angle scattering data and models.

12. Hura GL, Menon AL, Hammel M, Rambo RP, Poole FL 2nd , Tsutakawa SE, Jenney FE Jr, Classen S, Frankel KA, Hopkins RC et al.: Robust, high-throughput solution structural analyses by small angle X-ray scattering (SAXS). Nat Methods 2009, 6:606–612. [PubMed: 19620974]

13. Rambo RP, Tainer JA: Super-resolution in solution X-ray scattering and its applications to structural systems biology. Annu Rev Biophys 2013, 42:415–441. [PubMed: 23495971] • This review evaluates advances in computational and ensemble interpretations of biological scattering data and discusses hybrid structural refinement methods with NMR and single-molecule FRET.

14. Hura GL, Budworth H, Dyer KN, Rambo RP, Hammel M, McMurray CT, Tainer JA: Comprehensive macromolecular conformations mapped by quantitative SAXS analyses. Nat Methods 2013, 10:453–454. [PubMed: 23624664] •• Hura et al. introduce and benchmark the volatility-of-ratio (VR) metric for quantitative assessment of differences in paired SAXS curves and demonstrate its ability to detect conformational differences when clustered into SAXS similarity matrices (SSM) among different ligand states of the DNA repair factor MutSβ.

15. Chen PC, Hub JS: Interpretation of solution x-ray scattering by explicit-solvent molecular dynamics. Biophys J 2015, 108:2573–2584. [PubMed: 25992735] •• Chen and Hub describe the use of SWAXS-driven MD to guide explicit solvent all-atom molecular dynamics sampling restrained by solution scattering data. Their inclusion of explicit solvent avoids the need to parameterize fitting of the solvation layer or excluded solvent. Their technique captures ensemble conformations for the bacterial periplasmic protein LBP, pyrimidine synthesis enzyme aspartate carbamoyltransferase, and nuclear exportin CRM1.

16. Tang HYH, Tainer JA, Hura GL: High resolution distance distributions determined by X-ray and neutron scattering. Adv Exp Med Biol 2017, 1009:167–181. [PubMed: 29218559]

17. Solernou A, Hanson BS, Richardson RA, Welch R, Read DJ, Harlen OG, Harris SA: Fluctuating Finite Element Analysis (FFEA): a continuum mechanics software tool for mesoscale simulation of biomolecules. PLoS Comput Biol 2018, 14: e1005897. [PubMed: 29570700]

18. Rambo RP, Tainer JA: Bridging the solution divide: comprehensive structural analyses of dynamic RNA, DNA, and protein assemblies by small-angle X-ray scattering. Curr Opin Struct Biol 2010, 20:128–137. [PubMed: 20097063]

19. Parikh SS, Mol CD, Hosfield DJ, Tainer JA: Envisioning the molecular choreography of DNA base excision repair. Curr Opin Struct Biol 1999, 9:37–47. [PubMed: 10047578]

20. Stephens ZD, Lee SY, Faghri F, Campbell RH, Zhai C, Efron MJ, Iyer R, Schatz MC, Sinha S, Robinson GE: Big data: astronomical or genomical? PLoS Biol 2015, 13:e1002195. [PubMed: 26151137]

21. Franke D, Petoukhov MV, Konarev PV, Panjkovich A, Tuukkanen A, Mertens HDT, Kikhney AG, Hajizadeh NR, Franklin JM, Jeffries CM et al.: ATSAS 2.8: a comprehensive data analysis suite for small-angle scattering from macromolecular solutions. JAppI Crystallogr 2017, 50:1212–1225.•• An overview of the latest release (v. 2.8) of the ATSAS suite for SAXS data processing and analysis. Includes new tools for assessing the uniqueness and resolution of ab initio shape reconstruction solutions (AMBIMETER, DATCLASS, SASRES), analyzing SEC-SAXS data (CRHOMIXS), and interactive modeling in PyMOL (SASPy).

22. Hopkins JB, Gillilan RE, Skou S: BioXTAS RAW: improvements to a free open-source program for small-angle X-ray scattering data reduction and analysis. JAppI Crystallogr 2017, 50:1545–1553.

23. Broennimann C, Eikenberry EF, Henrich B, Horisberger R, Huelsen G, Pohl E, Schmitt B, Schulze-Briese C, Suzuki M, Tomizaki T et al.: The PILATUS 1M detector. J Synchrotron Radiat 2006, 13:120–130. [PubMed: 16495612]

24. Wernecke J, Gollwitzer C, Muller P, Krumrey M: Characterization of an in-vacuum PILATUS 1M detector. J Synchrotron Radiat 2014, 21:529–536. [PubMed: 24763642]

25. Perez J, Vachette P: A successful combination: coupling SE- HPLC with SAXS. Adv Exp Med Biol 2017, 1009:183–199. [PubMed: 29218560] • Overview of size-exclusion chromatography coupled SAXS (SEC-SAXS) with practical considerations for experimental set-up, sample preparation, and data processing and analysis.

26. Malaby AW, Chakravarthy S, Irving TC, Kathuria SV, Bilsel O, Lambright DG: Methods for analysis of size-exclusion chromatography-small-angle X-ray scattering and reconstruction of protein scattering. J Appl Crystallogr 2015, 48:1102–1113. [PubMed: 26306089]

27. Kirby NM, Cowieson NP: Time-resolved studies of dynamic biomolecules using small angle X-ray scattering. Current Opin Struct Biol 2014, 28:41–46.• Overview of time-resolved methods in biological X-ray scattering and experimental set-ups tailored to access different timescales, from femtoseconds to days.

28. Cho HS, Dashdorj N, Schotte F, Gräber T, Henning R, Anfinrud P: Protein structural dynamics in solution unveiled via 100-ps time-resolved x-ray scattering. Proc Natl Acad Sei USA 2010, 107:7281–7286.

29. Cho HS, Schotte F, Dashdorj N, Kyndt J, Henning R, Anfinrud PA: Picosecond photobiology: watching a signaling protein function in real time via time-resolved small- and wide-angle X-ray scattering. J Am Chem Soc 2016, 138:8815–8823. [PubMed: 27305463]

30. Meisburger SP, Taylor AB, Khan CA, Zhang S, Fitzpatrick PF, Ando N: Domain movements upon activation of phenylalanine hydroxylase characterized by crystallography and chromatography-coupled small-angle X-ray scattering. J Am Chem Soc 2016, 138:6506–6516. [PubMed: 27145334] • Meisburger et al. describe the application of Evolving Factor Analysis (EFA) to SEC-SAXS data to deconvolute scattering profiles of phenylalanine hydroxylase oligomers.

31. Round A, Felisaz F, Fodinger L, Gobbo A, Huet J, Villard C, Blanchet CE, Pernot P, McSweeney S, Roessle M et al.: BioSAXS sample changer: a robotic sample changer for rapid and reliable high-throughput X-ray solution scattering experiments. Acta Crystallogr D Struct Biol 2015, 71:67–75.

32. Schwemmer F, Blanchet CE, Spilotros A, Kosse D, Zehnle S, Mertens HDT, Graewert MA, Rossle M, Paust N, Svergun Dl et al.: LabDisk for SAXS: a centrifugal microfluidic sample preparation platform for small-angle X-ray scattering. Lab Chip 2016, 16:1161–1170. [PubMed: 26931639]

33. Rodriguez-Ruiz I, Radajewski D, Charton S, Phamvan N, Brennich M, Pernot P, Bonnete F, Teychene S: Innovative high-throughput SAXS methodologies based on photonic lab-on-a-chip sensors: application to macromolecular studies. Sensors 2017, 17:1266.
34. Grant TD, Luft JR, Carter LG, Matsui T, Weiss TM, Martel A,Snell EH: The accurate assessment of small-angle X-ray scattering data. Acta Crystallogr D Biol Crystallogr 2015, 71:45–56. [PubMed: 25615859]
35. Franke D, Kikhney AG, Svergun Dl: Automated acquisition and analysis of small angle X-ray scattering data. Nucl Instrum Methods Phys Res A 2012, 689:52–59.
36. Brosey CA, Ho C, Long WZ, Singh S, Burnett K, Hura GL, Nix JC, Bowman GR, Ellenberger T, Tainer JA: Defining NADH-driven allostery regulating apoptosis-inducing factor. Structure 2016, 24:2067–2079. [PubMed: 27818101]
37. Tainer JA, Getzoff ED, Alexander H, Houghten RA, Olson AJ, Lerner RA, Hendrickson WA: The reactivity of anti-peptide antibodies is a function of the atomic mobility of sites in a protein. Nature 1984, 312:127–134. [PubMed: 6209578]
38. Svergun Dl: Restoring low resolution structure of biological macromolecules from solution scattering using simulated annealing. Biophys J 1999, 76:2879–2886. [PubMed: 10354416]
39. Dl Svergun, Petoukhov MV, Koch MHJ: Determination of domain structure of proteins from X-ray solution scattering. Biophys J 2001, 80:2946–2953. [PubMed: 11371467]
40. Rambo RP, Tainer JA: Characterizing flexible and intrinsically unstructured biological macromolecules by SAS using the Porod-Debye law. Biopolymers 2011, 95:559–571. [PubMed: 21509745] •• Rambo and Tainer present the Porod-Debye interpretation of biomole-cular flexibility from I(q)·qn transforms of biological scattering data and use of the Porod exponent (PE) to objectively quantify changes in conformational flexibility. PE enables the use of the low angle SAXS data on small amounts of sample to distinguish disorder-to-order transitions from switching between discrete states.
41. Reyes FE, Schwartz CR, Tainer JA, Rambo RP: Methods for using new conceptual tools and parameters to assess RNA structure by small-angle X-ray scattering. Methods Enzymol 2014, 549:235–263. [PubMed: 25432752]
42. Rambo RP, Tainer JA: Accurate assessment of mass, models and resolution by small-angle scattering. Nature 2013,496:477–481. [PubMed: 23619693] •• Rambo and Tainer introduce new SAXS metrics for interpretation and model validation, including the volume-of-correlation (Vc) and its relationship to the power-law invariant (QR) for concentration-independent mass determination, and X2free and RSAS for model validation. Vc, which is the first SAXS invariant (model-independent parameter) discovered since the Porod invariant ~60 years ago, monitors a sample's thermodynamic state independently of its folding, unfolding, or concentration.
43. Hajizadeh NR, Franke D, Jeffries CM, Svergun Dl: Consensus Bayesian assessment of protein molecular mass from solution X-ray scattering data. Sci Rep 2018, 8:7204. [PubMed: 29739979]
44. Fischer H, Neto MD, Napolitano HB, Polikarpov I, Craievich AF: Determination of the molecular weight of proteins in solution from a single small-angle X-ray scattering measurement on a relative scale. J Appl Crystallogr 2010, 43:101–109.
45. Franke D, Svergun DI: DAMMIF, a program for rapid ab-initio shape determination in small-angle scattering. J Appl Crystallogr 2009, 42:342–346. [PubMed: 27630371]
46. Svergun DI: Restoring low resolution structure of biological macromolecules from solution scattering using simulated annealing. Biophys J 1999, 77 2896–2896.
47. Grant TD: Ab initio electron density determination directly from solution scattering data. Nat Methods 2018, 15:191–193. [PubMed: 29377013] • The novel ab initio shape reconstruction program DENSS uses iterative structure factor retrieval to determine low-resolution electron density envelopes directly from the scattering curve I(q), without assumptions of particle volume, shape, or occupancy. This approach improves ab initio modeling of regions of non-uniform electron density and multiple bio-molecular phases (protein, nucleic acid, lipid).
48. Petoukhov MV, Svergun DI: Ambiguity assessment of small- angle scattering curves from monodisperse systems. Acta Crystallogr D Biol Crystallogr 2015, 71:1051–1058. [PubMed: 25945570] • The program AMBlMETER assesses the uniqueness of a scattering curve I(q) by comparing its shape topology to an extensive library of pre-determined shape skeletons. The

comparison is summarized in a score that indicates the likelihood of nonambiguous shape reconstruction from the scattering data.

49. Tuukkanen AT, Svergun DI: Weak protein-ligand interactions studied by small-angle X-ray scattering. FEBS J 2014, 281:1974–1987. [PubMed: 24588935] • Tuukkanen et al. outline the strategy behind SASREF, which provides an assessment of ab initio model resolution based upon the degree of self-consistency within an ensemble of shapereconstructions.
50. Bernado P, Mylonas E, Petoukhov MV, Blackledge M, Svergun DI: Structural characterization of flexible proteins using small-angle X-ray scattering. J Am Chem Soc 2007, 129:5656–5664. [PubMed: 17411046]
51. Tria G, Mertens HDT, Kachala M, Svergun DI: Advanced ensemble modelling of flexible macromolecules using X-ray solution scattering. lUCrJ 2015, 2:207–217.
52. Pelikan M, Hura GL, Hammel M: Structure and flexibility within proteins as identified through small angle X-ray scattering. Gen Physiol Biophys 2009, 28:174–189.
53. Schneidman-Duhovny D, Hammel M, Tainer JA, Sali A: FoXS, FoXSDock and MultiFoXS: single-state and multi-state structural modeling of proteins and their complexes based on SAXS profiles. Nucleic Acids Res 2016, 44:W424–W429. [PubMed: 27151198]
54. Schneidman-Duhovny D, Hammel M, Tainer JA, Sali A: Accurate SAXS profile computation and its assessment by contrast variation experiments. Biophys J 2013, 105:962–974. [PubMed: 23972848]
55. Rozycki B, Kim YC, Hummer G: SAXS ensemble refinement of ESCRT-III CHMP3 conformational transitions. Structure 2011, 19:109–116. [PubMed: 21220121]
56. Yang S, Blachowicz L, Makowski L, Roux B: Multidomain assembled states of Hck tyrosine kinase in solution. Proc Natl Acad Sei USA 2010, 107:15757–15762.
57. Aceytuno RD, Piett CG, Havali-Shahriari Z, Edwards RA, Rey M, Ye RQ, Javed F, Fang SJ, Mani R, Weinfeld M et al.: Structural and functional characterization of the PNKP-XRCC4-LiglV DNA repair complex. Nucleic Acids Res 2017, 45:6238–6251. [PubMed: 28453785]
58. Banks A, Qin S, Weiss KL, Stanley CB, Zhou HX: Intrinsically disordered protein exhibits both compaction and expansion under macromolecular crowding. Biophys J 2018, 114:1067–1079. [PubMed: 29539394]
59. Kazantsev AV, Rambo RP, Karimpour S, Santalucia J Jr, Tainer JA, Pace NR: Solution structure of RNase P RNA. RNA 2011, 17:1159–1171. [PubMed: 21531920]
60. Leksa NC, Chiu PL, Bou-Assaf GM, Quan C, Liu Z, Goodman AB, Chambers MG, Tsutakawa SE, Hammel M, Peters RT et al.: The structural basis for the functional comparability of factor VIII and the long-acting variant recombinant factor VIII Fc fusion protein. J Thromb Haemost 2017, 15:1167–1179. [PubMed: 28397397]
61. Pretto DI, Tsutakawa S, Brosey CA, Castillo A, Chagot ME, Smith JA, Tainer JA, Chazin WJ: Structural dynamics and singlestranded DNA binding activity of the three N-terminal domains of the large subunit of replication protein A from small angle X-ray scattering. Biochemistry 2010, 49:2880–2889. [PubMed: 20184389]
62. Shi J, Nobrega RP, Schwantes C, Kathuria SV, Bilsel O, Matthews CR, Lane TJ, Pande VS: Atomistic structural ensemble refinement reveals non-native structure stabilizes a sub-millisecond folding intermediate of CheY. Sci Rep 2017, 7:44116. [PubMed: 28272524]
63. Kofinger J, Ragusa MJ, Lee IH, Hummer G, Hurley JH: Solution structure of the Atg1 complex: implications for the architecture of the phagophore assembly site. Structure 2015, 23:809–818. [PubMed: 25817386]
64. Remesh SG, Armstrong AA, Mahan AD, Luo J, Hammel M: Conformational plasticity of the immunoglobulin Fc domain in solution. Structure 2018, 28:1007–1014.
65. Schneidman-Duhovny D, Hammel M: Modeling structure and dynamics of protein complexes with SAXS profiles. Methods Mol Biol 2018, 1764:449–473. [PubMed: 29605933] • This methods paper provides a set-by-step overview of modeling protein complexes and dynamics from SAXS data and crystal structures with the Integrative Modeling Package (IMP) (with submodules FoXS and MultiFoXS), Modeller, and BILBOMD. The authors present three modelling protocols: (1) comparing solution and crystal structures, (2) multi-state modeling of a multidomain protein, and (3) protein-protein complex docking.

66. Chumnarnsilpa S, Robinson RC, Grimes JM, Leyrat C: Calcium-controlled conformational choreography in the N-terminal half of adseverin. Nat Commun 2015, 6:8254. [PubMed: 26365202]

67. Michael AK, Fribourgh JL, Chelliah Y, Sandate CR, Hura GL, Schneidman-Duhovny D, Tripathi SM, Takahashi JS, Partch CL: Formation of a repressive complex in the mammalian circadian clock is mediated by the secondary pocket of CRY1. Proc Natl Acad Sei USA 2017, 114:1560–1565.

68. Schwalbe M, Ozenne V, Bibow S, Jaremko M, Jaremko L,Gajda M, Jensen MR, Biernat J, Becker S, Mandelkow E et al.: Predictive atomic resolution descriptions of intrinsically disordered hTau40 and alpha-synuclein in solution from NMR and small angle scattering. Structure 2014, 22:238–249. [PubMed: 24361273]

69. Herranz-Trillo F, Groenning M, van Maarschalkerweerd A, Tauler R, Vestergaard B, Bernado P: Structural analysis of multi-component amyloid systems by chemometric SAXS data decomposition. Structure 2017, 25:5–15. [PubMed: 27889205] •• Herranz-Trillo et al. describe COSMiCS (Complex Objective Structural analysis of Multi-Component Systems), a unique data decomposition method that leverages multiple SAXS data representations (Kratky, Porod, Holtzer) to amplify distance-based differences among a mixture of species. The authors use COSMiCS analysis to deconvolve time-resolved, multi-species scattering data of insulin and α-synuclein fibrillation and to construct time courses of evolving populations during fibril formation.

70. Gahloth D, Dunstan MS, Quaglia D, Klumbys E, Lockhart-Cairns MP, Hill AM, Derrington SR, Scrutton NS, Turner NJ, Leys D: Structures of carboxylic acid reductase reveal domain dynamics underlying catalysis. Nat Chem Biol 2017, 13:975–981. [PubMed: 28719588]

71. Holdbrook DA, Burmann BM, Huber RG, Petoukhov MV, Svergun Dl, Hiller S, Bond PJ: A spring-loaded mechanism governs the clamp-like dynamics of the Skp chaperone. Structure 2017, 25:1079–1088. [PubMed: 28648612]

72. Tsutakawa SE, Yan CL, Xu XJ, Zhuang ZH, Washington MT, Tainer JA, Ivanov I: Structurally distinct ubiquitin- and SUMO-modified PCNA: implications for their distinct roles in the DNA damage response. J Biomol Struct Dyn 2015, 33:70–71. [PubMed: 24256122]

73. Tsutakawa SE, Van Wynsberghe AW, Freudenthal BD, Weinacht CP, Gakhar L, Washington MT, Zhuang ZH, Tainer JA, Ivanov I: Solution X-ray scattering combined with computational modeling reveals multiple conformations of covalently bound ubiquitin on PCNA. Proc Natl Acad Sei USA 2011, 108:17672–17677.

74. Hammel M, Yu Y, Mahaney BL, Cai B, Ye R, Phipps BM, Rambo RP, Hura GL, Pelikan M, So S et al.: Ku and DNA-dependent protein kinase dynamic conformations and assembly regulate DNA binding and the initial non-homologous end joining complex. J Biol Chem 2010, 285:1414–1423. [PubMed: 19893054]

75. Hammel M, Yu Y, Radhakrishnan SK, Chokshi C, Tsai MS, Matsumoto Y, Kuzdovich M, Remesh SG, Fang S, Tomkinson AE et al.: An intrinsically disordered APLF Links Ku, DNA-PKcs, and XRCC4-DNA ligaše IV in an extended flexible non-homologous end joining complex. J Biol Chem 2016, 291:26987–27006. [PubMed: 27875301] •• Hammel et al. use a combination of SEC-SAXS and ensemble modeling methods (BILBOMD-MES) to analyze NHEJ repair complexes. Application of SEC-SAXS ensures separation of intact, non-aggregating NHEJ assemblies away from unbound repair components and DNA substrate.

76. Hura GL, Tsai CL, Claridge SA, Mendillo ML, Smith JM, Williams GJ, Mastroianni AJ, Alivisatos AP, Putnam CD, Kolodner RD et al.: DNA conformations in mismatch repair probed in solution by X-ray scattering from gold nanocrystals. Proc Natl Acad Sei U S A 2013, 110:17308–17313.

77. Chen YJ, Tokuda JM, Topping T, Meisburger SP, Pabit SA, Gloss LM, Pollack L: Asymmetric unwrapping of nucleosomal DNA propagates asymmetric opening and dissociation of the histone core. Proc Natl Acad Sei USA 2017, 114:334–339. •• Chen et al. combine TR-SAXS with stopped-flow mixing and sucrose contrast matching to reveal changes in nucleosomal DNA conformation during salt-induced nucleosome disassembly. They use ensemble optimization methods to extract DNA conformations from TR-SAXS data and integrate these conformations with TR-FRET data to construct a kinetic scheme for nucleosome disassembly.

78. Chen YJ, Tokuda JM, Topping T, Sutton JL, Meisburger SP, Pabit SA, Gloss LM, Pollack L: Revealing transient structures of nucleosomes as DNA unwinds. Nucleic Acids Res 2014, 42:8767–8776. [PubMed: 24990379]

79. Plumridge A, Katz AM, Calvey GD, Elber R, Kirmizialtin S, Pollack L: Revealing the distinct folding phases of an RNA three-helix junction. Nucleic Acids Res 2018, 46:7354–7365. [PubMed: 29762712] •• Plumridge et al. use TR-SAXS and microfluidic mixing to study magnesium-induced folding of the tP5abc RNA three-helix junction from the Tetrahymena ribozyme. They identify characteristic ensembles of tP5abc conformations associated with each phase of folding by applying EOM to an RNA conformer pool derived from all-atom MD simulations. Their investigations identify distinct magnesium-driven collapse phases along the folding pathway.

80. Hub JS: Interpreting solution X-ray scattering data using molecular simulations. Curr Opin Struct Biol 2018, 49:18–26. [PubMed: 29172147]

81. Brosey CA, Yan CL, Tsutakawa SE, Heller WT, Rambo RP, Tainer JA, Ivanov I, Chazin WJ: A new structural framework for integrating replication protein A into DNA processing machinery. Nucleic Acids Res 2013, 41:2313–2327. [PubMed: 23303776]

82. Debiec KT, Whitley MJ, Koharudin LMI, Chong LT, Gronenborn AM: Integrating NMR, SAXS, and atomistic simulations: structure and dynamics of a two-domain protein. Biophys J 2018, 114:839–855. [PubMed: 29490245]

83. Weiel M, Reinartz I, Schug A: Rapid interpretation of small-angle X-ray scattering data. PLoS Comput Biol 2019, 15:e1006900. [PubMed: 30901335]

84. Pak AJ, Voth GA: Advances in coarse-grained modeling of macromolecular complexes. Curr Opin Struct Biol 2018, 52:119–126. [PubMed: 30508766]

85. Cheng P, Peng J, Zhang Z: SAXS-oriented ensemble refinement of flexible biomolecules. Biophys J 2017, 112:1295–1301. [PubMed: 28402873]

86. Bowerman S, Rana A, Rice A, Pham GH, Strieter ER, Wereszczynski J: Determining atomistic SAXS models of Tri-ubiquitin chains from Bayesian analysis of accelerated molecular dynamics simulations. J Chem Theory Comput 2017, 13:2418–2429. [PubMed: 28482663]

87. Yang KC, Rozycki B, Cui FC, Shi C, Chen WD, Li YQ: Sampling enrichment toward target structures using hybrid molecular dynamics-Monte Carlo simulations. PLoS One 2016, 11: e0156043. [PubMed: 27227775]

88. Shevchuk R, Hub JS: Bayesian refinement of protein structures and ensembles against SAXS data using molecular dynamics. PLos Comput Biol 2017, 13:e1005800. [PubMed: 29045407]

89. Grishaev A, Wu J, Trewhella J, Bax A: Refinement of multidomain protein structures by combination of solution small-angle X-ray scattering and NMR data. J Am Chem Soc 2005, 127:16621–16628. [PubMed: 16305251]

90. Grishaev A, Tugarinov V, Kay LE, Trewhella J, Bax A: Refined solution structure of the 82-kDa enzyme malate synthase G from joint NMR and synchrotron SAXS restraints. J Biomol NMR 2008, 40:95–106. [PubMed: 18008171]

91. Grishaev A, Ying J, Canny MD, Pardi A, Bax A: Solution structure of tRNAVal from refinement of homology model against residual dipolar coupling and SAXS data. J Biomol NMR 2008, 42:99–109. [PubMed: 18787959]

92. Knight CJ, Hub JS: WAXSiS: a web server for the calculation of SAXS/WAXS curves based on explicit-solvent molecular dynamics. Nucleic Acids Res 2015, 43:W225–W230. [PubMed: 25855813] • Accurate modeling of the solvent hydration layer and local thermal fluctuations complicate theoretical modeling of small-angle and wide-angle scattering data for high-resolution models. WAXSiS (WAXS in solvent) computes theoretical SWAXS curves based on explicit-solvent all-atom molecular dynamics (MD) simulations of the solvent layer, which provides more effective modeling of solvent hydration and of thermal contributions to the scattering curve.

93. Moore PB: The effects of thermal disorder on the solution-scattering profiles of macromolecules. Biophys J 2014, 106:1489–1496. [PubMed: 24703310]

94. Holton JM, Classen S, Frankel KA, Tainer JA: The R-factor gap in macromolecular crystallography: an untapped potential for insights on accurate structures. FEBS J 2014, 281:4046–4060. [PubMed: 25040949]

95. Jacob J, Krantz BA, Dothager RS, Thiyagarajan P, Sosnick TR: Early collapse is not an obligatory step in protein folding. Protein Sei 2004, 13 175–175.

96. de Oliveira GA, Silva JL: A hypothesis to reconcile the physical and chemical unfolding of proteins. Proc Natl Acad Sei USA 2015, 112:E2775–E2784.

97. Kathuria SV, Guo L, Graceffa R, Barrea R, Nobrega RP, Matthews CR, Irving TC, Bilsel O: Minireview: structural insights into early folding events using continuous-flow time-resolved small-angle X-ray scattering. Biopolymers 2011, 95:550–558. [PubMed: 21442608]

98. Konuma T, Kimura T, Matsumoto S, Goto Y, Fujisawa T, Fersht AR, Takahashi S: Time-resolved small-angle X-ray scattering study of the folding dynamics of barnase. J Mol Biol 2011, 405:1284–1294. [PubMed: 21146541]

99. Ogorzalek TL, Hura GL, Belsom A, Burnett KH, Kryshtafovych A, Tainer JA, Rappsilber J, Tsutakawa SE, Fidelis K: Small angle X-ray scattering and cross-linking for data assisted protein structure prediction in CASP 12 with prospects for improved accuracy. Proteins 2018, 86(Suppl. 1):202–214. [PubMed: 29314274]

100. Cinar S, Al-Ayoubi S, Sternemann C, Peters J, Winter R, Czeslik C: A high pressure study of calmodulin-ligand interactions using small-angle X-ray and elastic incoherent neutron scattering. Phys Chem Chem Phys 2018, 20:3514–3522. [PubMed: 29336441]

101. Lai YT, Hura GL, Dyer KN, Tang HY, Tainer JA, Yeates TO: Designing and defining dynamic protein cage nanoassemblies in solution. Sei Adv 2016, 2 e1501855. • Lai et al. benchmark protein nanocage assembly state and conformation using a simulated nanocage conformational landscape. The authors compare experimental scattering under diverse solvent pH and salt conditions to theoretical scattering profiles using high-throughput VR-based SAXS similarity analysis and force plots.

102. Behrouzi R, Roh JH, Kilburn D, Briber RM, Woodson SA: Cooperative tertiary interaction network guides RNA folding. Cell 2012, 149:348–357. [PubMed: 22500801]

103. Leamy KA, Yennawar NH, Bevilacqua PC: Cooperative RNA folding under cellular conditions arises from both tertiary structure stabilization and secondary structure destabilization. Biochemistry 2017, 56:3422–3433. [PubMed: 28657303]

104. Lipfert J, Sim AY, Herschlag D, Doniach S: Dissecting electrostatic screening, specific ion binding, and ligand binding in an energetic model for glycine riboswitch folding. RNA 2010, 16:708–719. [PubMed: 20194520]

105. Kilburn D, Behrouzi R, Lee HT, Sarkar K, Briber RM, Woodson SA: Entropie stabilization of folded RNA in crowded solutions measured by SAXS. Nucleic Acids Res 2016, 44:9452–9461. [PubMed: 27378777]

106. Roh JH, Guo L, Kilburn JD, Briber RM, Irving T, Woodson SA: Multistage collapse of a bacterial ribozyme observed by time-resolved small-angle X-ray scattering. J Am Chem Soc 2010, 132:10148–10154. [PubMed: 20597502]

107. Rambo RP, Tainer JA: Improving small-angle X-ray scattering data for structural analyses of the RNA world. RNA 2010, 16:638–646. [PubMed: 20106957]

108. Pollack L: Time resolved SAXS and RNA folding. Biopolymers 2011, 95:543–549. [PubMed: 21328311]

109. Jamros MA, Oliveira LC, Whitford PC, Onuchic JN, Adams JA, Blumenthal DK, Jennings PA: Proteins at work: a combined small angle X-ray scattering and theoretical determination of the multiple structures involved on the protein kinase functional landscape. J Biol Chem 2010, 285:36121–36128. [PubMed: 20801888]

110. Bothe JR, Tonelli M, AN IK, Dai ZQ, Frederick RO, Westler WM, Markley JL: The complex energy landscape of the protein IscU. Biophys J 2015, 109:1019–1025. [PubMed: 26331259]

111. Lee KK, Tsuruta H, Hendrix RW, Duda RL, Johnson JE: Cooperative reorganization of a 420 subunit virus capsid. J Mol Biol 2005, 352:723–735. [PubMed: 16095623]

112. Cordeiro TN, Chen PC, De Biasio A, Sibille N, Blanco FJ, Hub JS, Crehuet R, Bernado P: Disentangling polydispersity in the PCNA-p15PAF complex, a disordered, transient and multivalent macromolecular assembly. Nucleic Acids Res 2017, 45:1501–1515. [PubMed: 28180305] •• Cordeiro et al. characterize the transient and multivalent interaction between PCNA and its intrinsically disordered regulatory partner p15PAF by using MD-simulation derived

ensembles to globally fit multiple SAXS profiles collected across a titration series of the complex.

113. Pratt AJ, Shin DS, Merz GE, Rambo RP, Lancaster WA, Dyer KN, Borbat PP, Poole FL 2nd, Adams MW, Freed JH et al.: Aggregation propensities of superoxide dismutase G93 hotspot mutants mirror ALS clinical phenotypes. Proc Natl Acad Sei USA 2014, 111:E4568–E4576.
114. Chen PC, Hennig J: The role of small-angle scattering in structure-based screening applications. Biophys Rev 2018, 10:1295–1310. [PubMed: 30306530]
115. Brunette TJ, Parmeggiani F, Huang PS, Bhabha G, Ekiert DC, Tsutakawa SE, Hura GL, Tainer JA, Baker D: Exploring the repeat protein universe through computational protein design. Nature 2015, 528:580–584. [PubMed: 26675729]
116. Bale JB, Gonen S, Liu Y, Sheffler W, Ellis D, Thomas C, Cascio D, Yeates TO, Gonen T, King NP et al.: Accurate design of megadalton-scale two-component icosahedral protein complexes. Science 2016, 353:389–394. [PubMed: 27463675]
117. Fallas JA, Ueda G, Sheffler W, Nguyen V, McNamara DE, Sankaran B, Pereira JH, Parmeggiani F, Brunette TJ, Cascio D et al.: Computational design of self-assembling cyclic protein homo-oligomers. Nat Chem 2017, 9:353–360. [PubMed: 28338692]
118. Pesarrodona M, Crosas E, Cubarsi R, Sanchez-Chardi A, Saccardo P, Unzueta U, Rueda F, Sanchez-Garcia L, Serna N, Mangues R et al.: Intrinsic functional and architectonic heterogeneity of tumor-targeted protein nanoparticles. Nanoscale 2017, 9:6427–6435. [PubMed: 28463351]
119. Pham N, Radajewski D, Round A, Brennich M, Pernot P, Biscans B, Bonnete F, Teychene S: Coupling high throughput microfluidics and small-angle X-ray scattering to study protein crystallization from solution. Anal Chem 2017, 89:2282–2287. [PubMed: 28192906]
120. Joseph JS, Liu W, Kunken J, Weiss TM, Tsuruta H, Cherezov V: Characterization of lipid matrices for membrane protein crystallization by high-throughput small angle X-ray scattering. Methods 2011, 55:342–349. [PubMed: 21903166]
121. Greenswag AR, Muok A, Li XX, Crane BR: Conformational transitions that enable histidine kinase autophosphorylation and receptor array integration. J Mol Biol 2015, 427:3890–3907. [PubMed: 26522934]
122. Kalas V, Pinkner JS, Hannan TJ, Hibbing ME, Dodson KW, Holehouse AS, Zhang H, Tolia NH, Gross ML, Pappu RV et al.: Evolutionary fine-tuning of conformational ensembles in FimH during host-pathogen interactions. Sei Adv 2017, 3:e1601944.
123. Deshpande RA, Williams GJ, Limbo O, Williams RS, Kuhnlein J, Lee JH, Classen S, Guenther G, Russell P, Tainer JA et al.: ATP-driven Rad50 conformations regulate DNA tethering, end resection, and ATM checkpoint signaling. EMBO J 2014, 33:482–500. [PubMed: 24493214]
124. Chen PC, Masiewicz P, Rybin V, Svergun D, Hennig J: A general small-angle X-ray scattering-based screening protocol validated for protein-RNA interactions. ACS Comb Sei 2018, 20:197–202.
125. Tian X, Langkilde AE, Thorolfsson M, Rasmussen HB, Vestergaard B: Small-angle X-ray scattering screening complements conventional biophysical analysis: comparative structural and biophysical analysis of monoclonal antibodies lgG1, lgG2, and lgG4. J Pharm Sei 2014, 103:1701–1710.
126. Skamris T, Tian X, Thorolfsson M, Karkov HS, Rasmussen HB, Langkilde AE, Vestergaard B: Monoclonal antibodies follow distinct aggregation pathways during production-relevant acidic incubation and neutralization. Pharm Res 2016, 33:716–728. [PubMed: 26563206]
127. Mosbaek CR, Konarev PV, Svergun DI, Rischel C, Vestergaard B: High concentration formulation studies of an lgG2 antibody using small angle X-ray scattering. Pharm Res 2012, 29:2225–2235. [PubMed: 22477029]
128. Nishimura N, Hitomi K, Arvai AS, Rambo RP, Hitomi C, Cutler SRSchroeder Jl, Getzoff ED, : Structural mechanism of abscisic acid binding and signaling by dimeric PYR1. Science 2009, 326:1373–1379. [PubMed: 19933100]
129. Reindl S, Ghosh A, Williams GJ, Lassak K, Neiner T, Henche AL, Albers SV, Tainer JA: Insights into Flal functions in archaeal motor assembly and motility from structures, conformations, and genetics. Mol Cell 2013, 49:1069–1082. [PubMed: 23416110]

130. Guo HF, Tsai CL, Terajima M, Tan X, Banerjee P, Miller MD, Liu X, Yu J, Byemerwa J, Alvarado S et al.: Pro-metastatic collagen lysyl hydroxylase dimer assemblies stabilized by Fe2+-binding. Nat Commun 2018, 9:512. [PubMed: 29410444]

131. Christie JM, Arvai AS, Baxter KJ, Heilmann M, Pratt AJ, O'Hara A, Kelly SM, Hothorn M, Smith BO, Hitomi K et al.: Plant UVR8 photoreceptor senses UV-B by tryptophan-mediated disruption of cross-dimer salt bridges. Science 2012,335:1492–1496. [PubMed: 22323738]

132. Huang M, Song K, Liu X, Lu S, Shen Q, Wang R, Gao J, Hong Y, Li Q, Ni D et al.: Allofinder: a strategy for allosteric modulator discovery and allosterome analyses. Nucleic Acids Res 2018, 46:W451–W458. [PubMed: 29757429]

133. Bartuzi D, Kaczor AA, Matosiuk D: Opportunities and challenges in the discovery of allosteric modulators of GPCRs. Methods Mol Biol 2018, 1705:297–319. [PubMed: 29188568]

134. Moiani D, Ronato DA, Brosey CA, Arvai AS, Syed A, Masson J-Y, Petricci E, Tainer JA: Targeting allostery with avatars to design inhibitors assessed by cell activity: dissecting MRE11 endo-and exonuclease activities. Methods Enzymol 2018, 601:205–241. [PubMed: 29523233]

135. Ward AB, Sali A, Wilson IA: Biochemistry. Integrative structural biology. Science 2013, 339:913–915. [PubMed: 23430643]

136. van den Bedem H, Fraser JS: Integrative, dynamic structural biology at atomic resolution–it's about time. Nat Methods 2015, 12:307–318. [PubMed: 25825836]

137. Brosey CA, Ahmed Z, Lees-Miller SP, Tainer JA: What combined measurements from structures and imaging tell us about DNA damage responses. Methods Enzymol 2017, 592:417–455. [PubMed: 28668129]

138. Tsutakawa SE, Hura GL, Frankel KA, Cooper PK, Tainer JA: Structural analysis of flexible proteins in solution by small angle X-ray scattering combined with crystallography. J Struct Biol 2007, 158:214–223. [PubMed: 17182256]

139. Grishkovskaya I, Paumann-Page M, Tscheliessnig R, Stampler J, Hofbauer S, Soudi M, Sevcnikar B, Oostenbrink C, Furtmuller PG, Djinovic-Carugo K et al.: Structure of human promyeloperoxidase (proMPO) and the role of the propeptide in processing and maturation. J Biol Chem 2017, 292:8244–8261. [PubMed: 28348079]

140. Wallen JR, Zhang H, Weis C, Cui WD, Foster BM, Ho CMW, Hammel M, Tainer JA, Gross ML, Ellenberger T: Hybrid methods reveal multiple flexibly linked DNA polymerases within the bacteriophage T7 replisome. Structure 2017, 25:157–166. [PubMed: 28052235]

141. Williams RS, Moncalian G, Williams JS, Yamada Y, Limbo O, Shin DS, Groocock LM, Cahill D, Hitomi C, Guenther G et al.: Mre11 dimers coordinate DNA end bridging and nuclease processing in double-strand-break repair. Cell 2008, 135:97–109. [PubMed: 18854158]

142. Petoukhov MV, Svergun DI: Global rigid body modeling of macromolecular complexes against small-angle scattering data. Biophys J 2005, 89:1237–1250. [PubMed: 15923225]

143. Hennig J, Sattler M: The dynamic duo: combining NMR and small angle scattering in structural biology. Protein Sei 2014, 23:669–682.

144. Hennig J, Wang I, Sonntag M, Gabel F, Sattler M: Combining NMR and small angle X-ray and neutron scattering in the structural analysis of a ternary protein-RNA complex. J Biomol NMR 2013, 56:17–30. [PubMed: 23456097]

145. Whitley MJ, Xi Z, Bartko JC, Jensen MR, Blackledge M, Gronenborn AM: A combined NMR and SAXS analysis of the partially folded cataract-associated V75D YD-crystallin. Biophys J 2017, 112:1135–1146. [PubMed: 28355541]

146. Schwieters CD, Clore GM: Using small angle solution scattering data in Xplor-NIH structure calculations. Prog Nucl Magn Reson Spectrosc 2014, 80:1–11. [PubMed: 24924264]

147. Deshmukh L, Schwieters CD, Grishaev A, Ghirlando R, Baber JL, Clore GM: Structure and dynamics of full-length HIV-1 capsid protein in solution. J Am Chem Soc 2013, 135:16133–16147. [PubMed: 24066695]

148. Kulkarni P, Jolly MK, Jia DY, Mooney SM, Bhargava A, Kagohara LT, Chen YH, Hao PY, He YA, Veltri RW et al.: Phosphorylation-induced conformational dynamics in an intrinsically disordered protein and potential role in phenotypic heterogeneity. Proc Natl Acad Sei U S A 2017, 114: E2644–E2653.

149. Marsh JA, Forman-Kay JD: Ensemble modeling of protein disordered states: experimental restraint contributions and validation. Proteins 2012, 80:556–572. [PubMed: 22095648]

150. Thompson MK, Ehlinger AC, Chazin WJ: Analysis of functional dynamics of modular multidomain proteins by SAXS and NMR. Methods Enzymol 2017, 592:49–76. [PubMed: 28668130]

151. Betous R, Mason AC, Rambo RP, Bansbach CE, Badu-Nkansah A, Sirbu BM, Eichman BF, Cortez D: SMARCAL1 catalyzes fork regression and Holliday junction migration to maintain genome stability during DNA replication. Genes Dev 2012, 26:151–162. [PubMed: 22279047]

152. Pascal JM, Tsodikov OV, Hura GL, Song W, Cotner EA, Classen S, Tomkinson AE, Tainer JA, Ellenberger T: A flexible interface between DNA ligase and PCNA supports conformational switching and efficient ligation of DNA. Mol Cell 2006, 24:279–291. [PubMed: 17052461]

153. Forster F, Webb B, Krukenberg KA, Tsuruta H, Agard DA, Sali A: Integration of small-angle X-ray scattering data into structural modeling of proteins and their assemblies. J Mol Biol 2008, 382:1089–1106. [PubMed: 18694757]

154. Xu X, Yan C, Wohlhueter R, Ivanov I: Integrative modeling of macromolecular assemblies from low to near-atomic resolution. Comput Struct Biotechnol J 2015, 13:492–503. [PubMed: 26557958] •• This review highlights integrative computational approaches for modeling cryoEM and SAXS data. The authors discuss application of the molecular dynamics flexible fitting (MDFF) method for fitting crystal structures into cryoEM maps and Rosetta Monte-Carlo and MES methods for combining SAXS data with pseudoatomic structural models.

155. Webb B, Lasker K, Velazquez-Muriel J, Schneidman-Duhovny D, Pellarin R, Bonomi M, Greenberg C, Raveh B, Tjioe E, Russel D et al.: Modeling of proteins and their assemblies with the Integrative Modeling Platform. Methods Mol Biol 2014, 1091:277–295. [PubMed: 24203340] •• This methods article provides an overview of the Integrative Modeling Platform (IMP) for converting experimental structural and biochemical inputs into spatial information that can be used to generate integrative structural models of macromolecular complexes and assemblies.

156. Lossl P, van de Waterbeemd M, Heck AJ: The diverse and expanding role of mass spectrometry in structural and molecular biology. EMBO J 2016, 35:2634–2657. [PubMed: 27797822]

157. Faini M, Stengel F, Aebersold R: The evolving contribution of mass spectrometry to integrative structural biology. J Am Soc Mass Spectrom 2016, 27:966–974. [PubMed: 27056566]

158. Sinz A, Arlt C, Chorev D, Sharon M: Chemical cross-linking and native mass spectrometry: a fruitful combination for structural biology. Protein Sei 2015, 24:1193–1209.

159. Gomes GN, Gradinaru CC: Insights into the conformations and dynamics of intrinsically disordered proteins using singlemolecule fluorescence. Biochim Biophys Acta Proteins Proteomics 2017, 1865:1696–1706. [PubMed: 28625737]

160. Egelman EH: The current revolution in Cryo-EM. Biophys J 2016, 110:1008–1012. [PubMed: 26958874]

161. Elmlund D, Le SN, Elmlund H: High-resolution cryo-EM: the nuts and bolts. Curr Opin Struct Biol 2017, 46:1–6. [PubMed: 28342396]

162. Ekman AA, Chen JH, Guo J, McDermott G, Le Gros MA, Larabell CA: Mesoscale imaging with cryo-light and X-rays: larger than molecular machines, smaller than a cell. Biol Cell 2017, 109:24–38. [PubMed: 27690365]

163. Duke E, Dent K, Razi M, Collinson LM: Biological applications of cryo-soft X-ray tomography. J Microsc 2014, 255:65–70. [PubMed: 24942982]

164. Wagner J, Schaffer M, Fernandez-Busnadiego R: Cryo-electron tomography-the cell biology that came in from the cold. FEBS Lett 2017, 591:2520–2533. [PubMed: 28726246]

165. Rutsdottir G, Harmark J, Weide Y, Hebert H, Rasmussen Ml, Wernersson S, Respondek M, Akke M, Hojrup P, Koeck PJB et al.: Structural model of dodecameric heat-shock protein Hsp21: flexible N-terminal arms interact with client proteins while C-terminal tails maintain the dodecamer and chaperone activity. J Biol Chem 2017, 292:8103–8121. [PubMed: 28325834]

166. De Nardis C, Lossl P, van den Biggelaar M, Madoori PK, Leloup N, Mertens K, Heck AJ, Gros P: Recombinant expression of the full-length ectodomain of LDL receptor-related protein 1 (LRP1)

unravels pH-dependent conformational changes and the stoichiometry of binding with receptor-associated protein (RAP). J Biol Chem 2017, 292:912–924. [PubMed: 27956551]

167. Zhang Z, Liang WG, Bailey LJ, Tan YZ, Wei H, Wang A, Farcasanu M, Woods VA, McCord LA, Lee D et al.: Ensemble cryoEM elucidates the mechanism of insulin capture and degradation by human insulin degrading enzyme. eLife 2018, 7.
168. Hammel M, Amlanjyoti D, Reyes FE, Chen JH, Parpana R, Tang HY, Larabell CA, Tainer JA, Adhya S: HU multimerization shift controls nucleoid compaction. Sei Adv 2016, 2:e1600650.
169. Russel D, Lasker K, Webb B, Velazquez-Muriel J, Tjioe E, Schneidman-Duhovny D, Peterson B, Sali A: Putting the pieces together: integrative modeling platform software for structure determination of macromolecular assemblies. PLoS Biol 2012, 10:e1001244. [PubMed: 22272186]
170. Kim SJ, Fernandez-Martinez J, Nudelman I, Shi Y, Zhang W, Raveh B, Herricks T, Slaughter BD, Hogan JA, Upla P et al.: Integrative structure and functional anatomy of a nuclear pore complex. Nature 2018, 555:475–482. [PubMed: 29539637]
171. Sali A, Berman HM, Schwede T, Trewhella J, Kleywegt G, Burley SK, Markley J, Nakamura H, Adams P, Bonvin AM et al.: Outcome of the first wwPDB hybrid/integrative methods task force workshop. Structure 2015, 23:1156–1167. [PubMed: 26095030] • This report outlines recommendations and considerations for the reporting and curation of hybrid structural models, including guidelines for model representations, estimating model uncertainty, developing model archives, and publication standards.
172. Burley SK, Kurisu G, Markley JL, Nakamura H, Velankar S, Berman HM, Sali A, Schwede T, Trewhella J: PDB-Dev: a prototype system for depositing integrative/hybrid structural models. Structure 2017, 25:1317–1318. [PubMed: 28877501]
173. Chung PJ, Choi MC, Miller HP, Feinstein HE, Raviv U, Li YL, Wilson L, Feinstein SC, Safinya CR: Direct force measurements reveal that protein Tau confers short-range attractions and isoform-dependent steric stabilization to microtubules. Proc Natl Acad Sei USA 2015, 112:E6416–E6425.
174. Nishino Y, Eltsov M, Joti Y, Ito K, Takata H, Takahashi Y, Hihara S, Frangakis AS, Imamoto N, Ishikawa T et al.: Human mitotic chromosomes consist predominantly of irregularly folded nucleosome fibres without a 30-nm chromatin structure. EMBO J 2012, 31:1644–1653. [PubMed: 22343941] • This exemplary study uses a combination of cryoEM and SAXS to probe supramolecular structures formed by nucleosome fibers, revealing repetitive 10-nm fractal packaging, rather than the expected 30-nm organizing structure.
175. Maeshima K, Rogge R, Tamura S, Joti Y, Hikima T, Szerlong H, Krause C, Herman J, Seidel E, DeLuca J et al.: Nucleosomal arrays self-assemble into supramolecular globular structures lacking 30-nm fibers. EMBO J 2016, 35:1115–1132. [PubMed: 27072995]
176. Erdel F, Rippe K: Formation of chromatin subcompartments by phase separation. Biophys J 2018, 177:2262–2270.
177. Kedersha N, Ivanov P, Anderson P: Stress granules and cell signaling: more than just a passing phase? Trends Biochem Sei 2013, 38:494–506.
178. Stingle J, Bellelli R, Alte F, Hewiit G, Sarek G, Maslen SL, Tsutakawa SE, Borg A, Kjaer S, Tainer JA et al.: Mechanism and regulation of DNA-protein crosslink repair by the DNA-dependent metalloprotease SPRTN. Mol Cell 2016, 64:688–703. [PubMed: 27871365]
179. Cotner-Gohara E, Kim IK, Hammel M, Tainer JA, Tomkinson AE, Ellenberger T: Human DNA ligase III recognizes DNA ends by dynamic switching between two DNA-bound states. Biochemistry 2010, 49:6165–6176. [PubMed: 20518483]

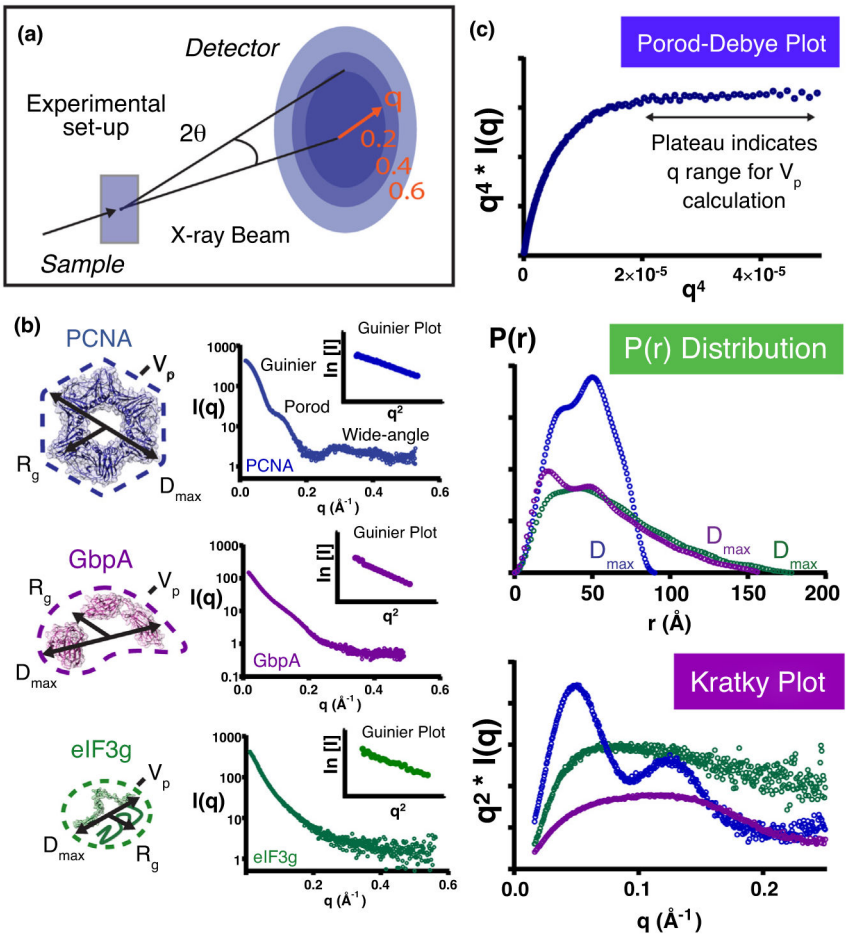

Figure 1. SAXS essentials-one experiment, many measurements.

(a) A single scattering experiment can provide multiple measures of macromolecular structure. In the basic SAXS experiment, macromolecular solutions are exposed to an X-ray beam, and scattered X-rays are recorded on a detector. Azimuthal integration of the recorded intensity at each q-value, subsequent subtraction of buffer scattering, and extrapolation to infinite dilution (to minimize effects of interparticle interference) yields the one-dimensional X-ray scattering profile, $I(q)$, that is used to probe molecular geometry and dynamics, **(b)** SAXS profiles are displayed for well-folded, oligomeric PCNA (purple, PDB: 1AXC, SASDBD7), modular GbpA (pink, PDB: 2XWX, SASDAA4), and disordered elF3g (green, PDB:4U1E). The scattering profiles of well-folded macromolecules exhibit elevations and dips (PCNA), while unfolded systems exhibit 'flat,' featureless scattering curves (elF3g). The scattering profile of GbpA, which contains ordered domains connected by flexible linkers, exhibits features that are smoothed. Linear transformation of the Guinier region of $I(q)$ (inset plots) provides an estimate of the radius-of-gyration (R_g). **(c)** Mathematical transformations of experimental $I(q)$ profiles yield additional structural information. The Porod-Debye transform is used to identify the scattering profile's Porod region for calculating the Porod volume (V_p) of well-folded macromolecules. Fourier transformation of $I(q)$ yields the real-space, paired-distance distribution, $P(r)$, with maximum dimension, D_{max}. The shape of the Kratky transform provides a qualitative assessment of the degree of

macromolecular folding or compactness. Well-folded macromolecules exhibit parabolic Kratky curves, which converge toward the baseline at high-q values (PCNA), while unfolded systems exhibit hyperbolic Kratky transforms (elF3g). The non-parabolic profile of modular GbpA reflects the flexibility of its linked domains.

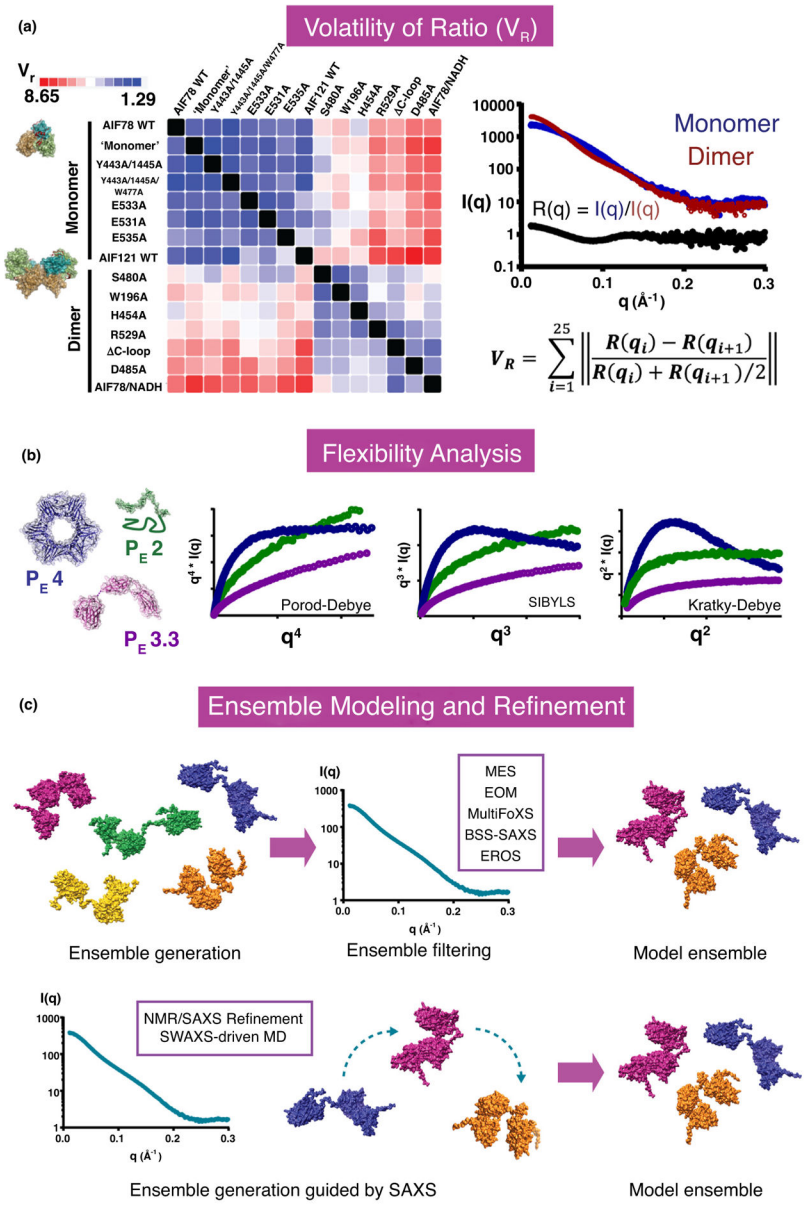

Figure 2. The expanding SAXS analysis toolbox: assessing similarity and biomolecular flexibility.

(a) Volatility of ratio (V_R). The Volatility-of-Ratio (Vr) metric quantifies high-resolution conformational differences between paired SAXS curves and importantly provides equal weighting between low-resolution and high-resolution g-space. High similarity follows low V_R values. Assembling V_R values into SAXS Similarity Matrices (SSM) and applying clustering routines reveals conformational populations, as shown for a library of mutants mimicking monomeric (blue) or dimeric (red) AIF (adapted with permission from Ref. [36]). **(b)** Flexibility Analysis. The Porod exponent (P_E) quantifies a power-law relationship describing the degree of foldedness versus flexibility in a sample. Complementary power transforms of the scattering curve by q^2, q^3, and q^4 enable detection of biomolecular flexibility. The well-defined PCNA architecture yields the maximum Porod exponent of 4 for a folded particle, reflected in the plateau of its Porod-Debye plot [$q^4 \cdot I(q)$] (purple trace).

In contrast, disordered elF3g exhibits the minimum Porod exponent of 2 for a flexible Gaussian coil, reflected in the plateau of its Kratky-Debye plot [$q^2 \cdot I(q)$] (green trace). Flexible, modular GpbA exhibits an intermediate Porod exponent of 3.3, reflecting its mixture of ordered domains and flexible linkers. For GbpA, plateaus are observed in all three power transforms at different q-ranges; for the q-range displayed here, plateaus are observed in the Kratky-Debye plot [$q^2 \cdot I(q)$] (pink trace). Plateau formation within the SIBYLS plots is particularly diagnostic for biomolecules that contain both ordered and disordered elements, **(c)** Ensemble Modeling and Refinement. Modeling conformational ensembles from SAXS data has traditionally been accomplished by screening conformers generated by simulation algorithms against the scattering profile, $I(q)$, to identify a grouping with the best fit to the data. SAXS-guided molecular dynamics (MD) simulations and hybrid NMR/SAXS refinement algorithms more robustly sample conformational space relevant to the ensemble by incorporating energy terms referencing the $I(q)$ scattering profile. Exemplary DNA Ligase III models and SAXS data were prepared with MultiFoXS [53,179] (PDB: 3L2P).

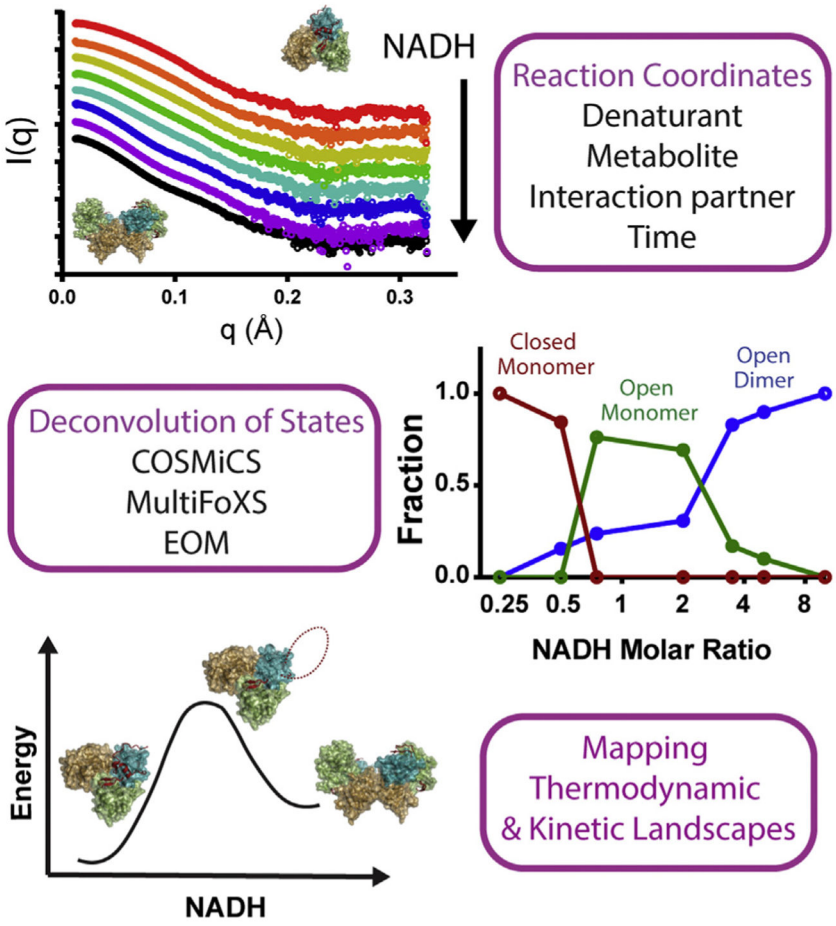

Figure 3. Illuminating biomolecular pathways and energy landscapes with SAXS.

The advent of multi-state modeling algorithms for deconvolution has enabled solution architectures to be transformed into reaction coordinates and energy landscapes. Sequential SAXS acquisition on macromolecules under evolving conditions of time, denaturant, metabolites, or binding partners can be analyzed for shifts in conformational populations, using known reference states (FoXS, EOM) or coordinate endpoints (COSMiCS). These evolving ensembles can subsequently be used to derive thermodynamic and kinetic insights on pathway progression. Here, SAXS monitors mitochondrial import and death factor protein AIF as it transitions from monomer to dimeric states upon binding NADH. Multi-state fitting with MultiFoXs identifies three populations: AIF monomer, AIF monomer with an internal 50-residue loop (C-loop) exposed to solvent, and AIF dimer with exposed C-loops.

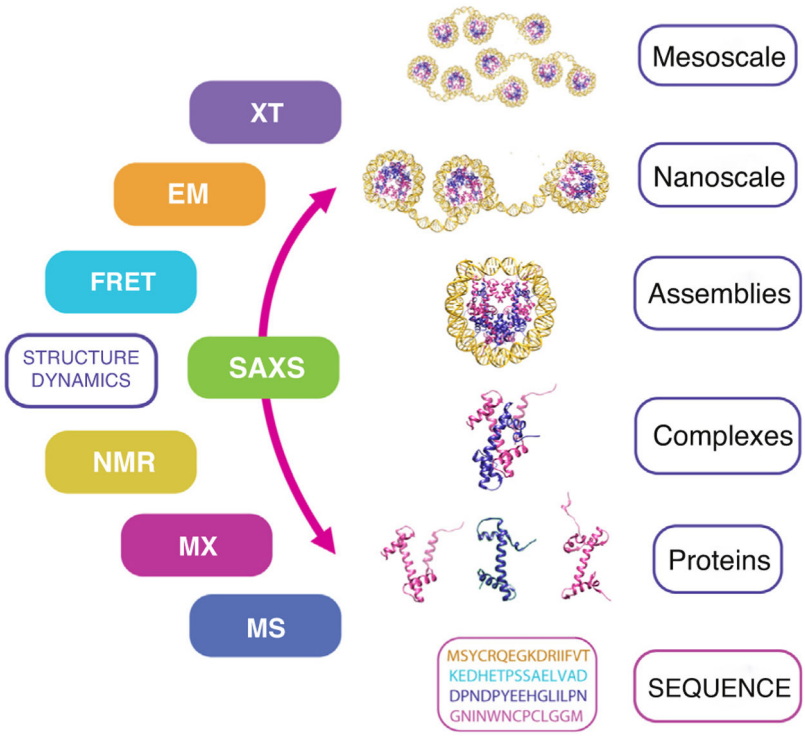

Figure 4. Integrative structural biology: moving from macromolecular assemblies to cellular structures.

The era of integrative structural biology brings multiple techniques to bear on multi-scale macromolecular structures, including X-ray tomography (XT), electron microscopy (EM), fluorescent resonance energy transfer (FRET), small-angle X-ray scattering (SAXS), nuclear magnetic resonance spectroscopy (NMR), macromolecular crystallography (MX), and mass spectrometry (MS). Structures of the human nucleosome adapted from PDB: 5AV8.